

UNCLASSIFIED

AD NUMBER
ADB278762
NEW LIMITATION CHANGE
TO Approved for public release, distribution unlimited
FROM Distribution authorized to U.S. Gov't. agencies only; Proprietary Info.; Sep 2001. Other requests shall be referred to U.S. Army Medical Research and Materiel Command, 504 Scott St., Ft. Detrick, MD 21702-5012.
AUTHORITY
USAMRMC ltr, 26 Nov 2002

THIS PAGE IS UNCLASSIFIED

AD _____

Award Number: DAMD17-00-1-0619

TITLE: The Use of Aptamers in Breast Cancer Anti-metastasis
Therapy

PRINCIPAL INVESTIGATOR: Bendicht U. Pauli, Ph.D.

CONTRACTING ORGANIZATION: Cornell University
Ithaca, New York 14853-2801

REPORT DATE: September 2001

TYPE OF REPORT: Final

PREPARED FOR: U.S. Army Medical Research and Materiel Command
Fort Detrick, Maryland 21702-5012

DISTRIBUTION STATEMENT: Distribution authorized to U.S. Government
agencies only (proprietary information, Sep 01). Other requests
for this document shall be referred to U.S. Army Medical Research
and Materiel Command, 504 Scott Street, Fort Detrick, Maryland
21702-5012.

The views, opinions and/or findings contained in this report are
those of the author(s) and should not be construed as an official
Department of the Army position, policy or decision unless so
designated by other documentation.

20020225 071

NOTICE

USING GOVERNMENT DRAWINGS, SPECIFICATIONS, OR OTHER DATA INCLUDED IN THIS DOCUMENT FOR ANY PURPOSE OTHER THAN GOVERNMENT PROCUREMENT DOES NOT IN ANY WAY OBLIGATE THE U.S. GOVERNMENT. THE FACT THAT THE GOVERNMENT FORMULATED OR SUPPLIED THE DRAWINGS, SPECIFICATIONS, OR OTHER DATA DOES NOT LICENSE THE HOLDER OR ANY OTHER PERSON OR CORPORATION; OR CONVEY ANY RIGHTS OR PERMISSION TO MANUFACTURE, USE, OR SELL ANY PATENTED INVENTION THAT MAY RELATE TO THEM.

LIMITED RIGHTS LEGEND

Award Number: DAMD17-00-1-0619
Organization: Cornell University

Those portions of the technical data contained in this report marked as limited rights data shall not, without the written permission of the above contractor, be (a) released or disclosed outside the government, (b) used by the Government for manufacture or, in the case of computer software documentation, for preparing the same or similar computer software, or (c) used by a party other than the Government, except that the Government may release or disclose technical data to persons outside the Government, or permit the use of technical data by such persons, if (i) such release, disclosure, or use is necessary for emergency repair or overhaul or (ii) is a release or disclosure of technical data (other than detailed manufacturing or process data) to, or use of such data by, a foreign government that is in the interest of the Government and is required for evaluational or informational purposes, provided in either case that such release, disclosure or use is made subject to a prohibition that the person to whom the data is released or disclosed may not further use, release or disclose such data, and the contractor or subcontractor or subcontractor asserting the restriction is notified of such release, disclosure or use. This legend, together with the indications of the portions of this data which are subject to such limitations, shall be included on any reproduction hereof which includes any part of the portions subject to such limitations.

THIS TECHNICAL REPORT HAS BEEN REVIEWED AND IS APPROVED FOR PUBLICATION.

Kath More 2/6/02

REPORT DOCUMENTATION PAGE

Form Approved
OMB No. 074-0188

Public reporting burden for this collection of information is estimated to average 1 hour per response, including the time for reviewing instructions, searching existing data sources, gathering and maintaining the data needed, and completing and reviewing this collection of information. Send comments regarding this burden estimate or any other aspect of this collection of information, including suggestions for reducing this burden to Washington Headquarters Services, Directorate for Information Operations and Reports, 1215 Jefferson Davis Highway, Suite 1204, Arlington, VA 22202-4302, and to the Office of Management and Budget, Paperwork Reduction Project (0704-0188), Washington, DC 20503

1. AGENCY USE ONLY (Leave blank)	2. REPORT DATE September 2001	3. REPORT TYPE AND DATES COVERED Final (1 Sep 00 - 31 Aug 01)
---	---	---

4. TITLE AND SUBTITLE The Use of Aptamers in Breast Cancer Anti-metastasis Therapy	5. FUNDING NUMBERS DAMD17-00-1-0619
--	---

6. AUTHOR(S)
Bendicht U. Pauli, Ph.D.

7. PERFORMING ORGANIZATION NAME(S) AND ADDRESS(ES)
Cornell University
Ithaca, New York 14853-2801

E-mail: hc26@cornell.edu

8. PERFORMING ORGANIZATION REPORT NUMBER

9. SPONSORING / MONITORING AGENCY NAME(S) AND ADDRESS(ES)
U.S. Army Medical Research and Materiel Command
Fort Detrick, Maryland 21702-5012

10. SPONSORING / MONITORING AGENCY REPORT NUMBER

11. SUPPLEMENTARY NOTES

12a. DISTRIBUTION / AVAILABILITY STATEMENT
Distribution authorized to U.S. Government agencies only (proprietary information, Sep 01). Other requests for this document shall be referred to U.S. Army Medical Research and Materiel Command, 504 Scott Street, Fort Detrick, Maryland 21702-5012.

12b. DISTRIBUTION CODE

13. ABSTRACT (Maximum 200 Words)
The objective of this one-year proposal was to initiate studies directed to identify and generate oligonucleotides (aptamers) that block the adhesion between tumor cell β_4 integrin and endothelial hCLCA2, an adhesion interaction implicated in pulmonary vascular arrest and metastasis of human breast cancer cells. Phase one of these studies was concerned with the generation of an "aptamer bait" for SELEX random sequence ssRNA library screening. Baits consisted of wild-type, full length β_4 protein, a polypeptide comprising the β_4 amino acids 108 to 343 (I-domain like structure), and a synthetic β_4 integrin-peptide representing the hCLCA2-binding domain. The first two "baits" proved to be useless due to poor harvest, insufficient purity, and loss of stability in case of full-length β_4 or insolubility of the 108-343 polypeptide prepared in insect cells. Identification of the hCLCA2-binding domain of β_4 was accomplished by domain swapping between the β_1 and β_4 integrins within the I-domain-like structure. A sequence of 20 amino acids was identified within that structure that harbors the hCLCA2-binding site. This sequence was synthesized and found to effectively block the β_4 integrin/hCLCA2 adhesion. Selection of aptamers is in progress using this promising, reproducible bait.

14. SUBJECT TERMS
Aptamer; B4 integrin; hCLCA2; breast cancer; metastasis;

15. NUMBER OF PAGES
29
16. PRICE CODE

17. SECURITY CLASSIFICATION OF REPORT
Unclassified

18. SECURITY CLASSIFICATION OF THIS PAGE
Unclassified

19. SECURITY CLASSIFICATION OF ABSTRACT
Unclassified

20. LIMITATION OF ABSTRACT
Unlimited

Table of Contents

Cover	1
SF 298	2
Table of Contents	3
Introduction	4
Body	5
Key Research Accomplishments	8
Reportable Outcomes	8
Conclusions	8
References	9
Appendices	10

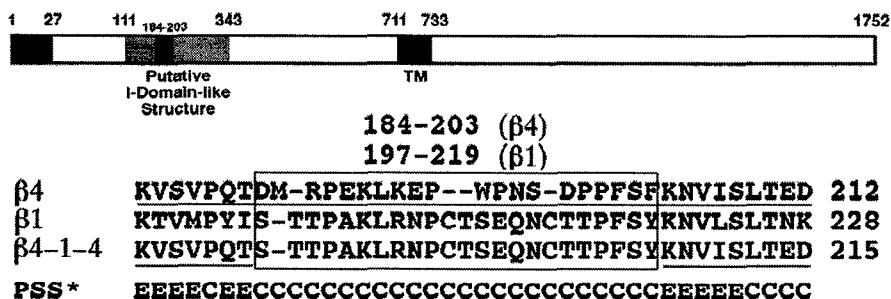
THE USE OF APTAMERS IN BREAST CANCER ANTI-METASTASIS THERAPY**INTRODUCTION**

The SELEX (systematic evolution of ligands by exponential enrichment) methodology, an *in vitro* protocol for isolating oligonucleotides (aptamers) that bind specifically and with high affinity and reproducibility to protein, is proposed to be used for the first time in producing compounds that block lung metastasis of breast cancer by interfering with the β_4 -integrin/ hCLCA2-mediated tumor cell/endothelial cell adhesion. The SELEX process begins with a starting pool of oligonucleotides (approximately 1×10^{17} ssRNA molecules/pool), each containing a 40-nucleotide randomized region that is nuclease-stabilized by using 2'-amino pyrimidine nucleotides for its synthesis and that is flanked by fixed sequences required for hybridization of primers and amplification by PCR. The random sequence ssRNA library is exposed here to myc-tagged human integrin β_4 ectodomain (amino acids 108 to 343) produced in insect cells and immobilized on nitrocellulose filters. Aptamers tightly bound to the protein target will be partitioned from the rest of the oligonucleotide pool, reverse transcribed, amplified, *in vitro* transcribed, and gel purified. The process of aptamer/target protein binding will be repeated for about 25 cycles. Evolving species of integrin β_4 -binding aptamers will be cloned and sequenced, and amplified RNA molecules tested for their ability to inhibit the adhesion between hCLCA2 and myc-tagged integrin β_4 ectodomain. Adhesion blocking aptamers will then be evaluated in cell adhesion assays and, ultimately, in lung colony assays in nude mice, using lung-metastatic MDA-MB-231 human breast cancer cells as test cells. This study represents a novel and highly promising approach to fighting often fatal breast cancer metastases.

BODY (STUDIES COMPLETED)

The original targets for identifying and isolating a β_4 /hCLCA2 adhesion inhibitory aptamer were full-length, wild-type β_4 integrin and a truncated β_4 ectodomain comprising amino acids 108 to 343 [$\beta_{4(108-343)}$: I-domain-like region]. The former was immunopurified from extracts of MDA-MB-231 human breast cancer cells as described by our laboratory (1), the latter from culture media of transfected insect cells. In brief, $\beta_{4(108-343)}$ -HA (partial influenza hemagglutinin sequence YPYDVPDYA) with *NotI* sites at the 5' and 3' prime ends was prepared by PCR, using human β_4 integrin cDNA as template. The PCR-fragment was then ligated into the *NotI* site of the baculovirus transfer vector pVL1392 (Invitrogen). The correct orientation and placement of the tag was confirmed by sequencing. A recombinant baculovirus containing $\beta_{4(108-343)}$ -HA cDNA was produced by homologous recombination in Sf-9 cells following co-transfection with the pVL1392/ $\beta_{4(108-343)}$ -HA construct and linear BaculoGold viral DNA, according to the manufacturer's protocol (Pharmingen) (2). Monolayers of 10^7 *Trichoplusia ni* cells were infected with plaque-purified recombinant virus at a multiplicity of infections of 10, then incubated with serum-free medium (IRL-41) supplemented with 0.4 mM ascorbic acid and antibiotics for 72 h (2,3). Recombinant $\beta_{4(108-343)}$ -HA was purified from culture media by adsorption to anti-HA mAb F-7 coupled to Protein A-agarose beads and eluted competitively with "epitope peptide" (0.1 to 1 mg/ml). Unfortunately, both of these techniques proved to be unsuitable in preparing an adequate bait for aptamer library screening. In case of wild-type β_4 integrin, the principal problems were poor harvest and insufficient purity of the β_4 -preparation (e.g., co-precipitation of the α_6 integrin), and in case of $\beta_{4(108-343)}$ -HA prepared in insect cells, the problem was solubility of the recombinant protein (most of the protein was insoluble even after digestion with 6M urea). Successful production of a bait was achieved only after identification of the hCLCA2 binding domain of the β_4 integrin. Our strategy of finding the CLCA2-binding domain in the β_4 integrin subunit was similar to that used for identifying the ligand binding domains of other β integrins such as β_1 and β_3 (4,5). These latter studies have led to the discovery that the ligand binding domain of β integrin subunits resides within an I-domain-like structure (e.g., this region spans amino acid residues 121 to 355 of β_1 and, correspondingly, residues 108 to 343 of β_4) (6,7) and that a diverse sequence within the putative I-domain-like structure of the β subunits accounts for their ligand binding specificity (5). Based on these data, we used overlap extension PCR technology to swap the putative ligand binding domain of the β_4 integrin (amino acid residues 184 to 203) with the corresponding domain in the β_1 integrin (amino acid residues 197 to 219), both located within a large predicted loop region that contains a nucleus that is not conserved among known integrin β subunits (5) (see Chart 1). After

Chart 1: Predicted Loop Region in β_4 Integrin I-Domain-like Structure



* Predicted Secondary Structure: E, sheet; C, coil.

verifying the mutation by sequencing and cloning of the construct β_{4-1-4} into a mammalian expression vector (pcDNA3.1/Zeo), it was stably transfected into α_6 -expressing MCF7 breast

cancer cells (control: MCF7 transfected with wild-type β_4 [wt β_4]). Surface expression was verified by immunoprecipitation (IP) of β_{4-1-4} (or wt β_4) from extracts of surface-biotinylated transfectants (Figure 1). Transfectant clones expressing equally prominent amounts of wt β_4 or β_{4-1-4} that both were co-precipitable with α_6 (using anti- α_6 mAbGoH3) were recently tested for adhesion to

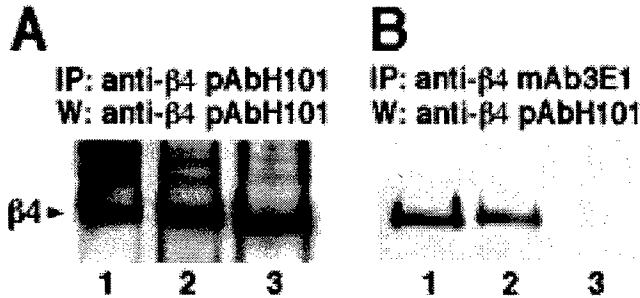


Figure 1: Western blots of anti- β_4 pAb H101- (A) or anti- β_4 mAb 3E1 (B) immunoprecipitates prepared from extracts of MDA-MB-231 (1), MCF7 transfected with wild-type β_4 (2), and MCF7 transfected with β_{4-1-4} (3) and probed with anti- β_4 pAb H101 (A & B) or anti- β_4 mAb 3E1 (B). Notice: mAb 3E1 is direct against the swapped region of the β_4 integrin.

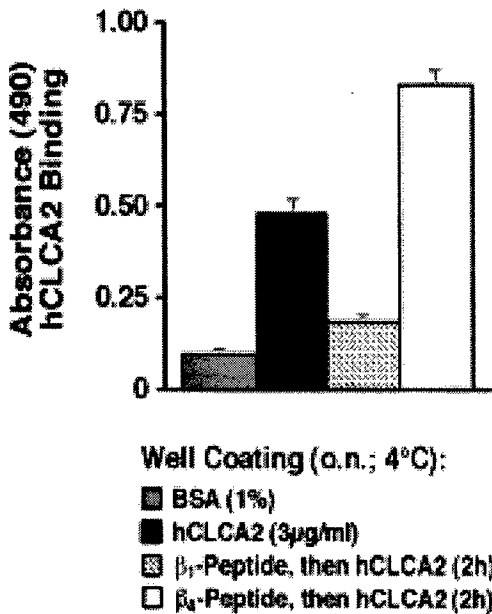


Figure 2: Binding of hCLCA2 to β_4 -peptide (swapped sequence): Wells of 96-well microtitration plates were coated with either BSA (1%), hCLCA2 (~3 μ g/ml), β_1 -peptide, or β_4 -peptide (2mg/ml) overnight (o.n.) at 4°C. Peptide-coated plates were then incubated with *Myc*-tagged hCLCA2 for 2h at 37°C. Bound hCLCA2 was detected with anti-*Myc* mAb 9E10 followed by goat anti-mouse IgG-HRP.

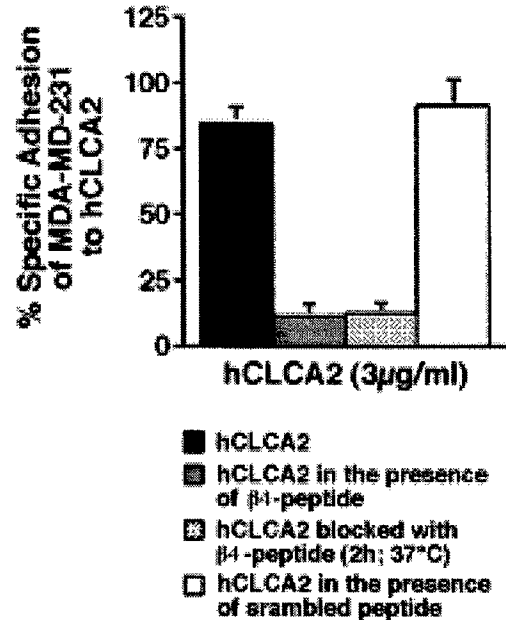


Figure 3: Inhibition of Adhesion of MDA-MB-231 breast cancer cells to hCLCA2 by β_4 -peptide (swapped sequence): Wells of 96-well microtitration plates were coated with hCLCA2 (~3 μ g/ml) overnight at 4°C. Wells were washed and blocked with 2.5% BSA, then seeded with MDA-MB-231 breast cancer cells (1×10^5 cells/well) in the absence (*black bar*) or presence of β_4 -peptide (β_4 -peptide present throughout adhesion assay: *gray bar*; β_4 -peptide incubated with hCLCA2-coated well for 2h at 37°C, then removed: *stippled bar*), or in the presence of corresponding β_1 peptide (*open bar*). The percent of tumor cells bound specifically to hCLCA2 was determined as described (1).

hCLCA2-coated microtitration plates. The selected MCF7-wt β_4 clone adhered to hCLCA2 ($62\pm 6\%$ specific adhesion), while the selected MCF7- β_{4-1-4} clone adhered at background levels to hCLCA2 (similar to untransfected MCF7 cells or vector-transfected cell clones: $10\pm 3\%$ specific adhesion). Correspondingly, a synthetic peptide comprising amino acids 184 to 203 of the β_4 integrin (swapped sequence) strongly bound hCLCA2 in ELISA (Figure 2) and totally blocked adhesion of MDA-MB-231 breast cancer cells to hCLCA2 (Figure 3), while the corresponding peptide sequence of the β_1 integrin and a scrambled peptide, respectively, had no effect (Figures 2 & 3).

The identified hCLCA2-binding domain of the β_4 integrin (double-cyclic, synthetic peptide of the β_4 integrin comprising amino acids 184 to 203) as it can be prepared in large, highly pure quantities. We are confident to complete screening of the aptamer library available in Dr. Lis' laboratory at Cornell University (see original application) and to amplify specifically bound aptamers by the end of the year. As a control peptide we will use a scrambled version of the β_4 -peptide as well as a synthetic peptide representing the corresponding region in the β_1 integrin (amino acids 197 to 219: this peptide has been examined and shown not to affect the binding of MDA-MB-231 to hCLCA2). Naturally, we will acknowledge support from the Army Research Institute (DoD) in future publications, although significant additional resources will be used to complete this very promising work.

KEY RESEARCH ACCOMPLISHMENTS

- Identification of the hCLCA2-binding domain on the β_4 integrin (swapping with corresponding sequence of the β_1 integrin abolishes adhesion of tumor cells transfected with swapped β_{4-1-4} to hCLCA2);
- Generation of synthetic peptide representing the hCLCA2-binding domain of the β_4 integrin;
- Establishment of binding specificity of synthetic peptide for hCLCA2 using ELISA (control: corresponding β_1 integrin peptide);
- Dose-dependent inhibition of the β_4 /hCLCA2 adhesion by synthetic peptide (control as above)
- Generation of monoclonal antibodies against the hCLCA2-binding domain of the β_4 integrin that exert significant anti-metastatic effects in nude mice injected with MDA-MB-231 cells

REPORTABLE OUCOMES

A manuscript describing the novel hCLCA2-binding sequence on the β_4 integrin of lung-metastatic human breast cancer cells is currently in preparation. In this manuscript, emphasis is on the unique anti-metastatic effects of (a) a synthetic peptide and (b) a monoclonal antibody generated against the hCLCA2-binding domain of the β_4 integrin. Both of these tools almost totally block hCLCA2-adhesion and prevent lung colonization of MDA-MB-231 human breast cancer cells. These data are supported by the above described transfection experiments, in which overexpression of the β_4 integrin was associated with increased lung-metastatic performance, while overexpression of the dominant negative β_{4-1-4} construct significantly decreased metastasis.

CONCLUSIONS

Using a variety of molecular techniques, we have identified the hCLCA2-binding domain on the β_4 integrin. Synthetic peptides and monoclonal antibodies generated against this domain have been shown to effectively block MDA-MB-231 breast cancer cell adhesion to hCLCA2 *in vitro* and lung-metastasis in nude mice. By identifying the hCLCA2-binding domain and by preparing a synthetic peptide against this domain, we believe to have generated a perfect bait for isolating oligonucleotides (aptamers) that specifically bind to the synthetic peptide sequence and, in addition, block the adhesion between the β_4 integrin and hCLCA2, thereby preventing lung metastasis of human breast cancer cells. Previously proposed baits (full-length β_4 integrin; β_4 ectodomain prepared in insect cells) proved to be ineffective as discussed in the "BODY" of the progress report, and their laborious preparation significantly delayed our progress in identifying functional aptamers. However, we are confident that in the next few months, we will be able to complete the proposed study, although funds for the project will be sparse.

REFERERENCES

1. Abdel-Ghany, M., Cheng, H.-C., Elble, R.C., and Pauli, B.U. The breast cancer β_4 integrin and endothelial hCLCA2 mediate lung metastasis. *J. Biol. Chem.* 276:25438-25446, 2001.
2. Murphy, C.I., Piwnica-Worms, H., Grünwald, S., and Romanow, W.G.: Expression and purification of recombinant proteins using the baculovirus system. In: *Current Protocols in Molecular Biology*, Ausubel, F.M., Brent, R., Moore, D.D., Seidman, J.G., Smith, J.A., and Struhl, K. (eds.), pp. 16.11.1-16.11.12, John Wiley & Sons, Inc., New York, 1994-1998.
3. McCormack, F.X., Damodarasamy, M., Elhalwagi, B.M.: Deletion mapping of N-terminal domains of surfactant protein A. *J. Biol. Chem.* 274:3173-3181, 1999.
4. Puzon-McLaughlin, W., and Takada, Y.: Critical residues for ligand binding in an I domain-like structure of the integrin $\beta 1$ subunit. *J. Biol. Chem.* 271:20438-20443, 1996.
5. Takagi, J., Kamata, T., Meredith J., Puzon-McLaughlin, W., and Takada, Y.: Changing ligand specificities of $\alpha v \beta 1$ and $\alpha v \beta 3$ integrins by swapping a short diverse sequence of the β subunit. *J. Biol. Chem.* 272:19794-19800, 1997.
6. Loftus, J.C., Smith, J.W., and Ginsberg, M.H.: Integrin-mediated cell adhesion: the extracellular face. *J. Biol. Chem.* 269:25235-25238, 1994.
7. Lee, J.-O., Rieu, P., Arnaout, M.A., and Liddington, R.: Crystal structure of the A domain from the α subunit integrin CR3 (CD11b/CD18). *Cell* 80:631-638, 1995.

Molecular cloning and transmembrane structure of hCLCA2 from human lung, trachea, and mammary gland

ACHIM D. GRUBER¹, KEVIN D. SCHREUR², HONG-LONG JI²,
CATHERINE M. FULLER,² AND BENDICHT U. PAULI¹

¹*Cancer Biology Laboratories, Department of Molecular Medicine,*

Cornell University College of Veterinary Medicine, Ithaca, New York 14853; and

²*Department of Physiology and Biophysics, University of Alabama, Birmingham, Alabama 35294*

Gruber, Achim D., Kevin D. Schreur, Hong-Long Ji, Catherine M. Fuller, and Bendicht U. Pauli. Molecular cloning and transmembrane structure of hCLCA2 from human lung, trachea, and mammary gland. *Am. J. Physiol.* 276 (*Cell Physiol.* 45): C1261–C1270, 1999.—The CLCA family of Ca²⁺-activated Cl⁻ channels has recently been discovered, with an increasing number of closely related members isolated from different species. Here we report the cloning of the second human homolog, hCLCA2, from a human lung cDNA library. Northern blot and RT-PCR analyses revealed additional expression in trachea and mammary gland. A primary translation product of 120 kDa was cleaved into two cell surface-associated glycoproteins of 86 and 34 kDa in transfected HEK-293 cells. hCLCA2 is the first CLCA homolog for which the transmembrane structure has been systematically studied. Glycosylation site scanning and protease protection assays revealed five transmembrane domains with a large, cysteine-rich, amino-terminal extracellular domain. Whole cell patch-clamp recordings of hCLCA2-transfected HEK-293 cells detected a slightly outwardly rectifying anion conductance that was increased in the presence of the Ca²⁺ ionophore ionomycin and inhibited by DIDS, dithiothreitol, niflumic acid, and tamoxifen. Expression in human trachea and lung suggests that hCLCA2 may play a role in the complex pathogenesis of cystic fibrosis.

calcium-activated chloride channel; cystic fibrosis

ION CHANNELS PLAY a crucial role in many diseases, most notably in cystic fibrosis, where a genetic defect of the cystic fibrosis transmembrane conductance regulator (CFTR) is responsible for the disturbed ion transport (3, 19, 23, 25, 26, 30). CFTR is a multifunctional transport protein that functions not only as an epithelial Cl⁻ channel but also as a regulator of other ion channels and cellular pathways (10, 29, 31). Several studies have indicated that, in addition to CFTR, a Ca²⁺-activated secretory pathway for Cl⁻ may play an important role in modulating the disease severity in various tissues of cystic fibrosis patients and CFTR knockout mice (1, 4, 18, 20, 27, 33, 35). However, little is known about the molecular basis of the channels involved.

A new family of proteins has recently been discovered that mediate a Ca²⁺-activated Cl⁻ conductance in a variety of tissues. Four members of this family have been identified, including bovine lung endothelial cell

adhesion molecule-1 (Lu-ECAM-1) (8, 40), bovine Ca²⁺-activated Cl⁻ channel (CaCC or bCLCA1) (6), murine CLCA1 (mCLCA1) (9), and human CLCA1 (hCLCA1) (11). Patch-clamp studies with transfected human embryonic kidney (HEK-293) cells have shown that bCLCA1, mCLCA1, and hCLCA1 mediate a Ca²⁺-activated Cl⁻ conductance that can be inhibited by the anion channel blocker DIDS and the reducing agent dithiothreitol (DTT). The protein size, structure, and processing seem to be similar among different CLCA family members and have been studied in most detail for Lu-ECAM-1 (8). The Lu-ECAM-1 open reading frame (ORF) encodes a precursor glycoprotein of 130 kDa that is processed to a 90-kDa amino-terminal cleavage product and a group of 30- to 40-kDa glycoproteins that are glycosylation variants of a single polypeptide derived from its carboxy terminus. Both subunits are associated with the outer cell surface, but only the 90-kDa subunit is thought to be anchored to the cell membrane via four transmembrane domains (8). Based on hydrophobicity analyses, analogous structural models have been suggested for mCLCA1 and hCLCA1 (9, 11). Although the protein processing and function appear to be conserved among CLCA homologs, significant differences exist in their tissue expression patterns. For example, bovine Lu-ECAM-1 is expressed primarily in vascular endothelia (40), bCLCA1 is exclusively detected in the trachea (6), and hCLCA1 is selectively expressed in a subset of human intestinal epithelial cells (11). Thus the emerging picture is that of a multigene family with members that are highly tissue specific, similar to the CIC family of voltage-gated Cl⁻ channels (14). A role for CLCA homologs in the complex ion-trafficking disorder of cystic fibrosis has been speculated, based on observations that the cellular expression patterns of bCLCA1, mCLCA1, and hCLCA1 overlap with that of CFTR in the respective tissues (6, 9, 11, 12). Before now no Ca²⁺-activated Cl⁻ channel had been cloned from human lung, the most severely affected organ in cystic fibrosis.

Here we describe the cloning of hCLCA2, the second hCLCA family member, and provide a detailed account of the membrane topology of this new Cl⁻ channel, using glycosylation site scanning and protease protection assays (28, 38). hCLCA2 is selectively expressed in lung, trachea, and mammary gland. Its transient expression in HEK-293 cells reveals a Ca²⁺-activated Cl⁻ conductance, which is similar to that of previously cloned CLCA family members.

The costs of publication of this article were defrayed in part by the payment of page charges. The article must therefore be hereby marked "advertisement" in accordance with 18 U.S.C. Section 1734 solely to indicate this fact.

MATERIALS AND METHODS

Isolation and cloning of the hCLCA2 cDNA. A human lung cDNA library (Clontech) was screened as described (11) using [α - 32 P]dCTP nick-labeled Lu-ECAM-1 cDNA as probe. For hybridization and washing, low-stringency conditions were applied [2 washes with $2\times$ standard sodium citrate (SSC), 0.1% SDS at 55°C for 20 min, followed by 2 washes with $0.4\times$ SSC, 0.1% SDS at 40°C for 10 min]. Positive phage clones were amplified, cloned into pBluescript (Stratagene), and sequenced. Automated sequencing with initial plasmid-derived primers followed by internal gene-specific primers was performed by the Cornell University DNA Sequencing Facility using dRhodamine terminator cycle sequencing on an ABI prism 377 DNA sequencer (PE Applied Biosystems). Missing 5' and 3' ends of the isolated cDNA species were completed using the rapid amplification of cDNA ends technique (RACE; Life Technologies). For expression studies, the 2,832-bp hCLCA2 ORF was PCR amplified from human trachea poly(A)⁺ RNA (Clontech) following reverse transcription with Superscript RNase H⁺ RT (Life Technologies) and random hexamer priming. PCR was performed with Pwo DNA polymerase [Boehringer; initial denaturation at 94°C for 3 min, 35 cycles at 94°C for 50 s, 58°C for 30 s, and 72°C for 2 min, with a time increment of 3 s/cycle for each extension step (72°C), followed by a final extension step of 72°C for 8 min]. Primer sequences were 5'-GCGGCCGCTACAA-CATGACCCAAAGGAGC-3' (upstream) and 5'-GCGGCCGCGACACTTTGGATATTTATTTATAATAATTTTGTTC-3' (downstream), with *Not* I linkers underlined. PCR products were gel purified, incubated with *Not* I, and cloned into the expression vector pcDNA3.1 (Invitrogen). Four different full-length PCR products were sequenced to control for potential PCR-induced sequence errors.

Northern blot and RT-PCR analyses. Human multiple tissue Northern blots (Clontech) contained 2 μ g poly(A)⁺ RNA per lane of heart, brain, placenta, lung, liver, skeletal muscle, kidney, pancreas, spleen, thymus, prostate, testis, ovary, small intestine, colon mucosa, peripheral blood leukocytes, stomach, thyroid, spinal cord, lymph node, trachea, adrenal gland, or bone marrow. In addition, total RNA was isolated (Trizol method, Life Technologies) from MCF-10A cells at 80% confluency (American Type Culture Collection). MCF-10A total RNA (20 μ g/lane) and human mammary gland poly(A)⁺ RNA (2 μ g/lane, Clontech) were resolved on a formaldehyde gel, blotted onto nitrocellulose, and hybridized with the [α - 32 P]dCTP nick-labeled (RTS RadPrime, Life Technologies) hCLCA2 cDNA as described (11). For the study on the hCLCA2 expression pattern, highly stringent washing conditions were employed (2 washes with $2\times$ SSC, 0.1% SDS at 55°C for 20 min followed by 2 washes with $0.1\times$ SSC, 0.1% SDS at 65°C for 20 min). Autoradiographs were exposed using an intensifying screen at -70°C for up to 8 days. Stripping of the blots and rehybridization with a probe for the housekeeping gene elongation factor-1 α (EF-1 α) were performed to control for RNA quality and loading amounts as described previously (13). RT-PCR was performed using the above-mentioned conditions and primers to detect hCLCA2 expression in poly(A)⁺ RNA samples from human lung, trachea, mammary gland, intestine, and spleen (Clontech) and in total RNA isolated from MCF-10A cells. PCR products were gel purified (QIAquick gel extraction kit; Qiagen), cloned into the pGem-T vector (Promega), and sequenced. In all RT-PCR assays, water, substituting for RNA in the reverse transcription, served as a negative control. A cDNA fragment of EF-1 α was amplified to control for conditions of reverse transcription and PCR (13).

In vitro translation, construction of glycosylation mutants, and protease protection assay. The hCLCA2 ORF cloned into the expression vector pcDNA3.1 was transcribed and translated with the TNT T7 coupled reticulocyte lysate system (Promega) in the presence of L-[35 S]methionine (Amersham). Reactions were carried out at 30°C for 90 min with and without canine pancreatic microsomal membranes (Promega). Samples were analyzed by 8% SDS-PAGE, followed by drying of the gel and exposure to film for 8 h.

Six cDNA constructs were generated with an asparagine (AAT or AAC) to glutamine (CAA) mutation that abolishes a consensus glycosylation site (NxS/T \rightarrow QxS/T). These mutations (N150Q, N292Q, N522Q, N637Q, N822Q, and N938Q) were positioned between adjacent potential transmembrane domains as determined by hydrophobicity analysis (Kyte-Doolittle algorithm, 19 amino acid residues per window). The constructs were generated by overlap extension PCR as described (11) and cloned into the *Not* I site of pcDNA3.1, using *Not* I site-incorporated PCR primers. Correct sequences of the products were verified by sequencing. The six constructs were in vitro translated in the absence or presence of microsomal membranes and resolved on an 8% ProSieve 50 Tris/glycine SDS-polyacrylamide gel (FMC Bioproducts) that enabled optimal resolution in the high-molecular-mass range. Molecular masses were estimated using molecular mass standards and a digital image analysis system (AlphaImager; AlphaInnotech). In addition, protease protection assays were performed as described (26). Briefly, in the presence of microsomal membranes in vitro translated and 35 S-labeled wild-type hCLCA2 was incubated with proteinase K (Sigma; 100 μ g/ml) for 60 min on ice with or without detergent present (0.5% Nonidet P-40). The reaction was stopped by adding 5 mM phenylmethylsulfonyl fluoride, and the products were analyzed by 12% SDS-PAGE, drying of the gel, and exposure to film.

Expression of Myc-tagged protein constructs in HEK-293 cells. Two Myc-tagged hCLCA2 constructs were generated by inserting a partial sequence of the human c-Myc protein (EQKLISEEDL) (5) near the amino or carboxy terminus of hCLCA2 (between amino acids 33 and 34 or 725 and 726), using overlap extension PCR as described (11), and cloned into pcDNA3.1. Correct sequences were verified by sequencing. DNA constructs were transfected into 70% confluent HEK-293 cells via the Lipofectamine Plus method (Life Technologies) using 20 μ l Plus reagent, 30 μ l lipid, and 4 μ g DNA/100-mm dish in a 3-h incubation. Cells were lysed 48 h later in the presence of protease inhibitors (1% aprotinin, 1 μ M leupeptin, 2 mM phenylmethylsulfonyl fluoride). Lysates were resolved via 10% SDS-PAGE, blotted, and probed with mouse anti-human c-Myc antibody 9E10 (Calbiochem), followed by enhanced chemiluminescence detection (ECL; Amersham). Surface expression of the proteins was shown by surface biotinylation (Biotin NHS, Vector; 100 μ g/ml) of transfected nonpermeabilized HEK-293 cells 48 h after transfection (20 min at 37°C, followed by extensive washing with PBS). Immunoprecipitation with antibody 9E10, incubation with protein G beads, boiling of the beads in SDS loading buffer, and SDS-PAGE were followed by blotting and detection with peroxidase-conjugated streptavidin and ECL. To estimate the extent of hCLCA2 glycosylation, 9E10 immunoprecipitates were incubated with *N*-glycanase (0.3 U/40 μ l sample; Genzyme) at 37°C for 18 h before sample denaturation and loading of the gel.

Electrophysiology. The hCLCA2 cDNA was transiently transfected into HEK-293 cells, which lack an endogenous Ca²⁺-activated Cl⁻ conductance (9, 11, 41). To control for transfection efficiency and to identify transfected cells, the

same cells were cotransfected with a green fluorescent protein reporter vector (EGFP, Clontech). Parental HEK-293 cells were cultured in DMEM with 10% fetal bovine serum in the absence of antibiotics. Cells grown on collagen-coated glass coverslips placed in the bottom of 35-mm dishes were transfected with 5 μ l Lipofectamine, 0.5 μ g of hCLCA2 cloned into pcDNA3.1, and 0.5 μ g of EGFP during a 2- to 3-h incubation period (Life Technologies). After transfection, cells were allowed to recover for 24 h before patch-clamp recording. In all cases, the cells that were cotransfected with hCLCA2 and EGFP and that fluoresced green were also expressing a Ca^{2+} -sensitive Cl^- conductance, whereas no currents were observed in mock-transfected (EGFP alone) or untransfected cells (see also Refs. 9 and 11). To record channel activities under whole cell conditions, cells were superfused at 1–2 ml/min with bath solution (in mM: 112 *N*-methyl-D-glucamine chloride, 30 sucrose, 2 $CaCl_2$, 2 $MgCl_2$, and 5 HEPES, pH 7.4). Borosilicate glass electrodes (tip resistance 6–9 M Ω) were filled with an identical solution plus 5 mM ATP. In some experiments designed to examine the effect of 4 μ M ionomycin, the pipette solution also contained 1 mM EGTA and 0.366 mM $CaCl_2$. The free Ca^{2+} concentration under these conditions was calculated to be \sim 25 nM. After seal formation ($>$ 1 G Ω) and establishment of the whole cell recording configuration, cells were clamped at +20 mV and currents recorded at room temperature using an Axopatch 200A (Axon Instruments, Foster City, CA) connected to a personal computer through a TL1 interface (Axon) with 12-bit resolution. The records were sampled at 5–10 kHz and filtered at 1–2 kHz with a four-pole Bessel filter. The current-voltage relationship of hCLCA2 was determined using 300-ms voltage steps from a holding potential of +20 mV to potentials from –100 to +100 mV at 10-mV intervals. To normalize membrane currents for differences in cell size, the capacitive current transiently recorded in response to a 10-mV hyperpolarizing pulse was integrated and divided by the given voltage to give total membrane capacitance for each cell.

Nucleotide sequence accession number. The GenBank accession number for the hCLCA2 sequence is AF043977.

RESULTS

Identification and cloning of hCLCA2. A human lung cDNA library was screened with Lu-ECAM-1 cDNA as probe in an attempt to isolate a CLCA homolog from human lung. After the sequencing of the positive clones and completion of the 5' and 3' cDNA ends by the RACE technique, a single 3.6-kb cDNA species was identified and named hCLCA2. Sequence accuracy was verified by sequencing of four different full-length RT-PCR products from human trachea mRNA generated by the highly accurate Pwo DNA polymerase. The nucleotide sequence shared high degrees of identity with those of Lu-ECAM-1 (86%), bCLCA1 (85%), mCLCA1 (76%), and hCLCA1 (63%). Northern blot analyses under highly stringent conditions yielded bands of the expected size of 3.6 kb in trachea and mammary gland, whereas all other tissues tested were negative (Fig. 1). Although isolated from a lung cDNA library, hCLCA2 was not detected in the lung by Northern blot hybridization. However, the more sensitive RT-PCR revealed its expression in lung in addition to trachea and mammary gland, suggesting a significantly lower expression level in the lung. Because of RNA analyses from whole tissue extracts, the cell types expressing hCLCA2 could not be identified. However, hCLCA2 was also detected in the nonmalignant human mammary epithelial cell line MCF-10A using both Northern blot and RT-PCR analyses (Fig. 1), suggesting epithelial expression at least in the mammary gland. All PCR products were sequenced, and sequence identities with the cDNA isolated from

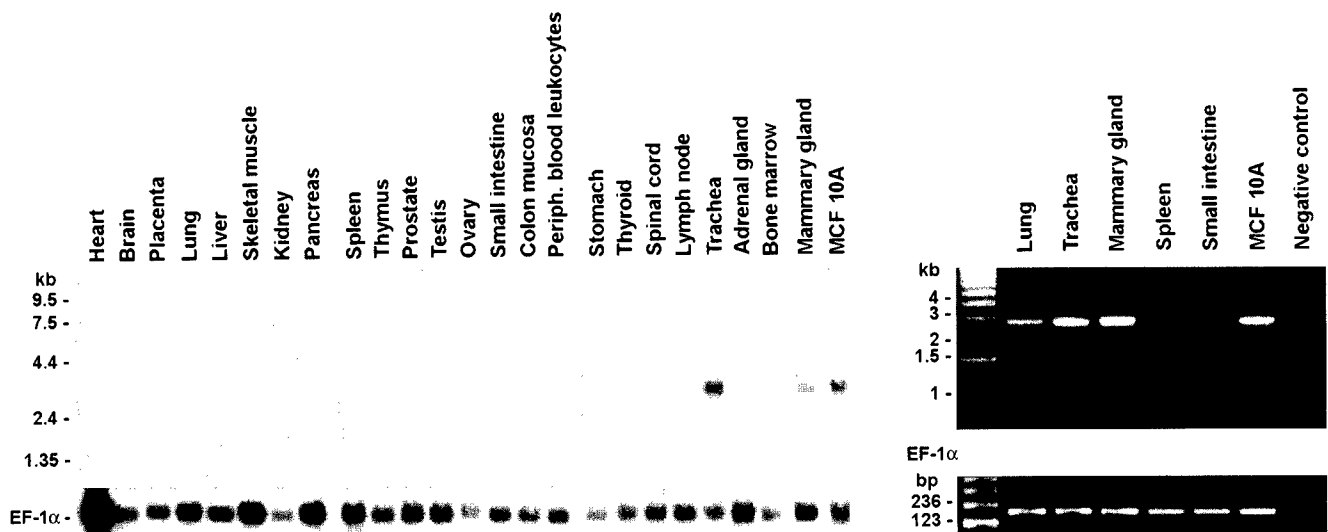


Fig. 1. Northern blot hybridization and RT-PCR analyses of hCLCA2 tissue expression pattern. Poly(A)⁺ RNA (2 μ g/lane) from human tissues and mammary epithelial cell line MCF-10A was hybridized with a ³²P-labeled probe representing the hCLCA2 open reading frame (ORF; *top left*). Absence of a signal for intestinal hCLCA1 indicates specificity for hCLCA2. Blots were stripped and rehybridized with a probe for elongation factor-1 α (EF-1 α) as an internal control (*bottom left*). Exposure times were 48 h (hCLCA2) and 24 h (EF-1 α). *Top right*: RT-PCR analysis of hCLCA2 expression in human tissues and cell line MCF-10A with primers flanking entire ORF (2,838 bp). A 219-bp fragment of EF-1 α was amplified to control for RNA quality and RT-PCR conditions (*bottom right*). Negative controls starting from reverse transcription included sterile water instead of RNA.

the lung library together with the observed signal size of 3.6 kb on the RNA blots indicated that both the RNA blot and RT-PCR signals in fact represented hCLCA2.

Characterization of the hCLCA2 protein. The ORF of the hCLCA2 cDNA encodes a 943-amino acid polypeptide with high levels of amino acid sequence identity with Lu-ECAM-1 (76%), bCLCA1 (76%), mCLCA1 (69%), and hCLCA1 (51%; Fig. 2). The polypeptide is preceded by a canonical signal sequence with a predicted signal peptidase cleavage site between amino acids 31 and 32 (32). The predicted size of the full-length protein (104 kDa) is consistent with the results of an *in vitro* translation assay yielding a primary translation product of ~105 kDa (Fig. 3A). In the presence of microsomal membranes, the protein was glycosylated *in vitro* to a 120-kDa glycoprotein. To ascertain whether the hCLCA2 protein is cleaved into two subunits in mammalian cells as reported for other CLCA homologs (8, 9, 11), two cDNA constructs were generated with a c-Myc tag within the amino or carboxy terminus, respectively (constructs "m1" and "m2") and transfected into HEK-293 cells. In fact, immunoblots of cell lysates probed with an anti-Myc antibody identified an 86-kDa protein when the tag was inserted near the amino terminus (m1) and a 34-kDa protein when the tag was situated near its carboxy terminus (m2; Fig. 3B), confirming a similar cleavage in hCLCA2. The presence of protease inhibitors in the lysis buffer suggests that the observed cleavage did not occur after lysis of the cells. To study the extent of glycosylation of each subunit, immunoprecipitates of both Myc-tagged constructs from transfected HEK-293 cells were deglycosylated by *N*-glycanase treatment. The 86- and 34-kDa glycoproteins were reduced in size by 11 and 2.5 kDa, proposing approximately four and one glycosylation sites, respectively (Fig. 3B). Detection of the two Myc-tagged constructs in anti-Myc antibody immunoprecipitates from surface-biotinylated, nonpermeabilized HEK-293 cells suggests that both the 86- and 34-kDa proteins are expressed on the surface of the transfected cells (Fig. 3C).

To elucidate the transmembrane topology of hCLCA2, glycosylation site scanning and protease protection assays were performed as described for other channel proteins (28, 38). Potential transmembrane regions were determined using a hydrophobicity analysis (Fig. 4). Based on this prediction, six glycosylation knockout cDNA constructs were generated, each having a single asparagine-to-glutamine (N→Q) mutation that abolishes a consensus glycosylation site between two adjacent potential transmembrane domains (N150Q, N292Q, N522Q, N637Q, N822Q, and N938Q). Following *in vitro* translation and glycosylation, the products were analyzed using a high-resolution PAGE. Mutation of three of the six sites (N150Q, N522Q, and N822Q) led to a reduction in size of the respective glycoproteins by ~2 kDa, indicating usage of these sites and therefore extracellular location (Fig. 3A). However, lack of size reduction of the remaining constructs did not necessarily prove intracellular location of their mutated sites, because an extracellular consensus glycosylation site

may not have been used due to sterical hindrance. Therefore, a protease protection assay was performed to determine the sizes of the extracellular domains, complementing the information derived from the glycosylation site scanning. In principle, extracellular loops are protected from proteolysis due to their translocation into the lumen of lipid microsomes, functionally representing the endoplasmic reticulum. The calculated sizes of each possible extracellular domain of hCLCA2 are given in Fig. 4 with ~2 kDa to be added per adjacent transmembrane domain. Wild-type hCLCA2 was *in vitro* translated in the presence of microsomal membranes and digested with proteinase K in the absence or presence of detergent. Three degradation products of 18, 21, and 30 kDa were protected from proteolysis in the absence of detergent (Fig. 3A), indicating their extension into the microsomes. In the presence of detergent, the protein was fully degraded. Both the glycosylation data and the sizes of protected extracellular domains are consistent with a five-transmembrane topology (Fig. 5). In the proposed model, the fragments protected from proteolysis correspond in size to the first extracellular domain (30 kDa, resulting from 27.7 kDa plus one transmembrane segment, tm1), the second extracellular domain (18 kDa, resulting from 13.7 kDa plus two transmembrane segments, tm2 and tm3), and the third extracellular domain (21 kDa, resulting from 16.8 kDa plus two transmembrane segments, tm4 and tm5). The size of the 21-kDa fragment also indicates degradation and therefore intracellular location of the carboxy-terminal tail of ~2 kDa. Given the number and locations of consensus glycosylation sites of the primary hCLCA2 polypeptide (Fig. 2), this transmembrane model is also consistent with the extent of glycosylation of the two 86- and 34-kDa subunits as detected by *N*-glycanase treatment (Fig. 3B). Accordingly, the 86-kDa subunit contains three glycosylation sites within the first (N74, N97, and N150) and one within the second extracellular loop (N522), whereas only one site (N822) is present within the extracellular loop of the 34-kDa cleavage product (Fig. 5).

When compared with the amino acid sequences of previously cloned homologs, hCLCA2 shares a number of interesting sequence motifs. For example, the pattern of cysteine residues present within the large amino-terminal, extracellular domain of all previously cloned homologs is conserved in hCLCA2 (Fig. 2). Also conserved is the consensus site for monobasic proteolytic cleavage following arginine residue 675 (7), the location of which is consistent with the sizes of the cleavage products of 86 and 34 kDa. Analyses of the predicted intracellular domains of hCLCA2 revealed seven consensus phosphorylation sites for protein kinase C (PKC; Fig. 5) but none for Ca²⁺/calmodulin protein kinase II or cAMP-dependent protein kinase.

Electrophysiological characterization of hCLCA2. Electrophysiological studies for hCLCA2 were conducted in a manner analogous to those reported for bCLCA1, mCLCA1, and hCLCA1, which have all been shown to be associated with activation of a Ca²⁺-

		<u>S</u>		
h CLCA2	MTQRSTAGPFCNLFVTLILVALSSELPFLGAGVQLQDNGYNGLLIAINPQVPENQNLISNIKEMITEASFYLFNATKRRV			80
h CLCA1	.GPFKVS-----VFIL.I.HL-.E.GA.S--NSLI.NN...E.IVV..D.N...DET..QQ..D.V.Q..L...E..GK.F			72
b CLCA1	.VP.LTV-----IL.L.HL-.PG-MK---SSM.N.IN...D.IV.....S...DEK..Q...V...T...H.....			71
Lu-ECAM-1	.VLCNV-----IL.L.HL-.PG-MK---SSM.N.IN...D.IV.....S...DEK..E...V...T...H.....			71
m CLCA1	.VPGLQV-----L.L.HL-.QN-TE---SSM.H.NS...E.VV.....S...DER..PS...V.Q..T...E..SQG..			71
h CLCA2	FFRNIKILIPATWKANN--SKIKQESYEKANVIVTDWYGAHGDPPYTLQYRGCGKEGKYIHFTPNFLLNDLNTAGYGSRG			159
h CLCA1	Y.K.VA...E...TKADYVRP.L.T.KN.D.L.AESTPPGN.E...E.MGN..EK.ER..L..D.IAGKK.AE--..PQ.			151
b CLCA1	Y...VS...M...SKSEYLMP...DQ.E...ANP.LK.....GR..EK.Q.....TN..PI.....			150
Lu-ECAM-1	Y...VS...M...SKSEYFIP...DQ.D...ANP.LKY.....GR..EK.....TN.FHI.....			150
m CLCA1	Y...S...V.M...SKSEYLMP.R...D..D...A.PHLQ.....GQ..DR.Q.....T...RI...P..			150
h CLCA2	RVFVHEWAHLRWGVFDEYNNDKPFYINGNQIKVTRCSDIDITGIFV---CEKGPCEQENCISK---LFEKGCFTIYNS			232
h CLCA1	KA.....EK..LS-NGR.QAV...AG...TN.V-KK.OG.S.YTKR.TFN.VTG.YEK..E.VLQ.			229
b CLCA1	.A.....I.....G.Q...SRR.T.EA...TH...TN.IVK-.QG.S.ITRP.RRDSQTG.YEAK...PEK			229
Lu-ECAM-1I.....V.Q...SRK.T.EA...TH...N.VFKK.PG.S.ITSL.RRDSQTG.YEAK...LPKK			230
m CLCA1V.R...SRK.T.EA...AS...KK.V-HE.QR.S.VTRA.RRDSKTR.YEPK...PDK			229
h CLCA2	TQNATASIMFMQSLSSVVEFCNASTHNQEPNLQNMCSLRSAWDVI TDSADFHHSFPMNGTELPPPTFLVQAGDKVV			312
h CLCA1	R.TEK....A.HVD.I...TEQN..K...K...K.N...T.E.R.E..KKT.TT--Q.N...L.I.QRI.			307
b CLCA1	S.T.RE....H...T...TEK...V...K..NGK.T...MN.T...QNTS..TEMNP.TQ.....LKSQR.			309
Lu-ECAM-1	S.T.KE....P.H.T...TEK...T...K..NGK.T...MN.V..QNTS..TEMNP.TH...LKSQR.			310
m CLCA1	I.T.G....N.N...TENN..A...K..NR..T...KT...QNAP..R...A...Y.LKSRRR..			309
h CLCA2	CLVLDVSSKMAEADRLQLQQAEEFLMQLIVEIHTFVGIASFDSKGEIRAQLHQINSNDRKLLVSYLPTTVSAKTDISI			392
h CLCA1K.GS..TGN..NR.N..GQLF.L.T..LGSW..MVT...AAHVQSE.I...GS..DT.AKR..AA--..SGGT.			385
b CLCA1K.GS.SSE...FRMN...LF.I..I.KGSL..MVT...VA..NN.TK.TDDNVYENITAN..QE--..NGGT.			387
Lu-ECAM-1K.GS.SAE...F.MN...L.I..VI.KGSL..MVT...VA..QNH.TR.TDDNVYQKITAK..QV--..NGGT.			388
m CLCA1K.GS.DKE...IRMN...L..T...KESM..LVT...AAH.QNY.IK.T.SS.YQKITAN..QQ--..SGGT.			387
h CLCA2	CSGLKKGFEVVEKLNKAYGSVMILVTSGDGKLLGNCLPTVLSSGSTIHSIALGSSAAPNLEELSRLTGGLKFFVDPDISN			472
h CLCA1	...RSA.-T.IRKKYPTD..EIV.L.D.E.NTISG.FNE.KQ..AI..TV...P...QE...KM...QTYAS.QVQ			464
b CLCA1	.R...A..QAIHQSQSTS..EI..L.D.E.NEIH.S.IEE.KQ..VI..T...P...KE..T..DM...HR.YANKDI-			466
Lu-ECAM-1	.R...A..QAIHQSQSTS..EI..L.D.E.NEIRS.FED.KR..AI..T...P...KE..T..NM...YR.YANKDI-			467
m CLCA1	.H...QA..QAITSSDQSTS..EIV.L.D.E.NEIRS.FEA.SR..AI..T...P.R.RE..T..DM...R.YANKDL-			466
h CLCA2	SNSMIDAFSRISSGTGDIHQHIQLESTGENVKKPHQLKNTVTVDNTVGN*TMFLVTWQASGPPEIILFDPGRKYTNN			552
h CLCA1	N.GL...GAL...N.AVS.RS...K.LTLQNSQWMNG..I..S...K..L..I..-TTQ..Q.L.W..S.Q..-OGG			541
b CLCA1	-.GLTN...RS.S.T..T...KALAITKQWVNG..P.S.I...F.V...-TIKK...L.Q..K.K..K.SD			544
Lu-ECAM-1	-TGLTN...RS.S.T..A...KALKITGRKRVNG..P.S...F.V...-TIQK...V.Q..K.K..K.SD			545
m CLCA1	-.L.L...TS.SVS..AL...KAFD.RAGAWING..PL.S...F.VI..-MVKK...Q..K.K..T.SD			544
h CLCA2	FITN-LTFRASLWIPGTAKPGHWYTLNTHHSLQALKVTVTSRASNSAVPPATVEAFVERDSLHPHPVMIYANVKQG			631
h CLCA1	.VVDK-NTKM.Y.Q...I..V.T.K.S---QA.S.T.TL...ATL..I..TSKTNK.TSK..S.LVV...IR.			617
b CLCA1	.KEDK.NIHS.R.R...I.ET.T...S.L.N.A.P.I.T...T..RSPTT.V.AT.HMSQNTA.Y.S..IV..Q.S..			624
Lu-ECAM-1	.KEDK.NI.S.R.Q...I.ET.T...S.L.N.A.S.M.T...T..RSPTI..VIAT.HMSQHTA.Y.S.MIV..Q.S..			625
m CLCA1	.QDDK.NI.S.R.Q...ET.T...SY--GTKS.LITM...T..RSPTME.LLGYCYMSQSTAQY.SRMIV..R.S..			622
h CLCA2	FYPILNATVTVTATVEPETGDPVTLRLDLDGAGADVIKNDGIYSRYFFSFAANGRYSLKVHVHNSPISITPAHSIPGSHAMY			711
h CLCA1	AS...R.S...LI.SVN.KT...E...N...AT.D.V...TTDYT...V..RALGGVNAARRRVIPOQ.G.L			697
b CLCA1	.L.V.GIN..II.T.D.HQ...E.W.N...TV...TDYRG...AEARNNTARLNSLRQ.QNK.L			704
Lu-ECAM-1	.L.V.GIS.I.II.T.D.HQ...E.W.N...R.TV...TDYYG...AQARNNTARLNSLRQ.QNKVL			705
m CLCA1	.L.V.G.N...LI.A.H.HQ...E.W.N...IV...T...TDYHG...R.QAQRNKTRELNSLRQ-KNKSL			701
h CLCA2	VPGYTANGNIQMNAPRKSVMGRNEERKVG-FSRVSSGGSFVSLG-VPAGPHPDVFPCKIIDLEA-VKVEELTSLWTAP			788
h CLCA1	I..WIE.DE..W.P..PEINKDDVQH.QVC..T.....-ASD..NA.I..L..GQ.T..K.EIHGGSLIN.T...			776
b CLCA1	I...IE..K.I.L.P..PE.KDDLAKAELED..LT...T.S.AP..N.S.L.N...KF.ED-HIQ.....			782
Lu-ECAM-1	...VE..K.I.L.P..PE.KDDLAKA.IED..LT...T.S.AP.P.N.S...S.T...KF.ED-YIQ.....			784
m CLCA1	I...VE..K.VL.P..PD.QEEAI.ATVED.N..T...T.S.AP.D.D.AR...S.VT...EFIGD-YIH.T...			780
h CLCA2	GEDFDQGQATSYEIRMSKSLQNIQDDFNNAIIVNTSKRNPQAGIREIFTFSPQISTNGPEHPNGETHESHRIYVAIRA			868
h CLCA1	.D.Y.H.T.HK.I...I.T.ILDLR.K..ESLQ...TALI..KE.NSE.V.L.K.ENI.....FENGTDLFI..Q			846
b CLCA1	ANVL.K.K.N..I..I...FLDL.K..D..T...SLK.KE..SD.N.E.K.EPFR-----IENGTNF.I.VQ			852
Lu-ECAM-1	.NVL.K.K.N..I..I...FMDR.E..D..T...NLI.KE..SK.N.E.K.EHFR-----VENGTNF.ISVQ			854
m CLCA1	.KVL.N.R.HR.I...QHPLDL.E...T...A.SLI.KE..SK.A.K.K.ETFK-----IANGIQL.I..Q			850
h CLCA2	MDRNSLQASVSNIAQAPLFIIPNSDP-VPARDYLKGLVLTAMGLIGIICLIIVVTHHTLSRKRKRADKKEGNTKLL			943
h CLCA1	V.KVD.K.EI...RVS...QTP.ET.SP-----ETSAPCPN..H.NST.PGIHILKIMW.WIG---LQLSIA			914
b CLCA1	INEAN.T.E...IK...MP-----EDSVP.L.-TK.SAINLAIFALAMI-----LSIV			904
Lu-ECAM-1	INEAN.I.E..H.V..IK..LP-----EDSVHDL.-TK.SEITLAILGLPMI-----FSV-F			905
m CLCA1	DNEA..T.E...VKLTSL-----EDSIS.L.-DD.SAISMTIWGL.VI-----FNSI.N			902

Fig. 2. Predicted hCLCA2 amino acid sequence aligned (Clustal method) with all known CLCA homologs. Identical amino acids are indicated by dots; dashes represent gaps. Major hydrophobic regions spanning 19 or more amino acid residues are overlined (S, signal sequence; 1-5, transmembrane domains). Cysteine residues conserved in amino-terminal extracellular domain are bold and enlarged. Consensus sites are marked for N-linked glycosylation (*), phosphorylation by protein kinase C (PKC) (:), and phosphorylation by cAMP-dependent protein kinase (■). Arrow, conserved consensus site for monobasic proteolytic cleavage; ::, 2 adjacent PKC sites. GenBank accession numbers are AF039400 (hCLCA1), U36455 (bCLCA1 or CaCC), AF001261 (Lu-ECAM-1), and AF047838 (mCLCA1). Lu-ECAM-1, lung endothelial cell adhesion molecule-1; h, human; b, bovine; m, murine.

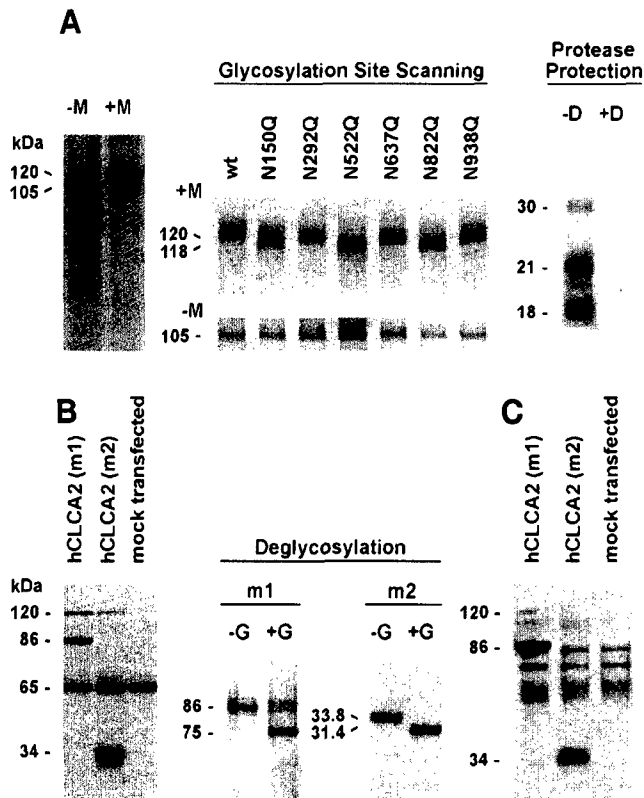


Fig. 3. Biochemical analysis of the hCLCA2 protein. **A:** in vitro translation without (-M) and with (+M) processing and glycosylation by microsomal membranes. Glycosylation site scanning was performed by in vitro translation of 6 glycosylation knockouts [N150Q to N938Q; wild type (wt)]. Unglycosylated constructs uniformly ran at 105 kDa (-M), whereas glycosylated proteins were 120 kDa (wt, N292Q, N637Q, N938Q) or 118 kDa (N150Q, N522Q, N822Q) in size (+M; 8% gel). In a protease protection assay, three fragments of 18, 21, and 30 kDa were protected from degradation by proteinase K in absence of detergent (-D), and the polypeptide was fully degraded in presence of detergent (+D; 12% gel). In all experiments, L-[³⁵S]methionine-labeled proteins were detected by SDS-PAGE, drying of the gel, and exposure to film for 8 h. **B:** immunoblot detection of Myc-tagged hCLCA2 constructs overexpressed in HEK-293 cells. Tags were placed near the amino terminus (m1) or within the carboxy-terminal cleavage product (m2; see Fig. 5). The 120-kDa precursor protein was processed into 2 proteins of 86 kDa (m1) and 34 kDa (m2). The somewhat weaker band below the 34-kDa band (2nd lane) probably represents an incomplete glycosylation variant of this protein, which may not be visible in the less abundant 120-kDa precursor due to lower resolution in the high-molecular-mass range of this blot. Bands at 65 and 67 kDa represent endogenous c-Myc. Cell lysates including protease inhibitors were resolved by 10% SDS-PAGE 48 h after transfection, transferred to a membrane, and probed with anti-Myc antibody 9E10. Deglycosylation with N-glycanase (+G) reduced the molecular masses from 86 to 75 kDa (m1) and from 33.8 to 31.4 kDa (m2). **C:** analysis of surface expression of Myc-tagged hCLCA2 constructs m1 and m2. Transfected HEK-293 cells were surface biotinylated, washed extensively with PBS, and lysed in the presence of protease inhibitors, followed by immunoprecipitation with anti-Myc antibody 9E10, SDS-PAGE, and probing with horseradish peroxidase-conjugated streptavidin. Both the 86- and 34-kDa proteins were biotinylated and therefore associated with the apical cell membrane.

sensitive Cl⁻ conductance. When transiently expressed in HEK-293 cells, hCLCA2 was associated with an outwardly rectified current that was activated by ionomycin. In contrast, nontransfected cells, cells transfected with the EGFP vector alone (mock-transfected),

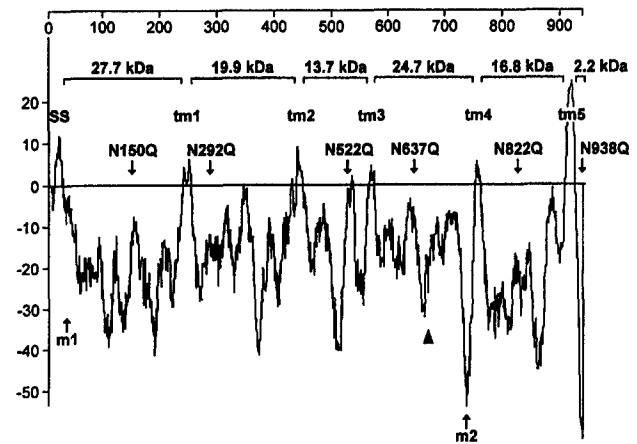


Fig. 4. Hydrophobicity plot of hCLCA2 amino acid sequence (Kyte-Doolittle algorithm, 19 amino acid residues/window). Hydrophobic domains are given as positive values (SS, signal sequence; tm1 to tm5, transmembrane regions). Numbers and bars above curve indicate calculated molecular masses between transmembrane domains, including 2 kDa per potential glycosylation site for interpretation of results of protease protection assay. Names of glycosylation knockouts (NxQ) indicate locations of their abolished glycosylation sites. Sites where a Myc tag was placed in constructs m1 and m2 are indicated with arrows under curve. Arrowhead, consensus site for monobasic proteolytic cleavage. Units are in kcal/mol (vertical axis) and first amino acid residue/window (horizontal axis).

or transfected cells in the absence of ionomycin were not associated with any significant current (Fig. 6). The outwardly rectifying current-voltage relationship exhibited by hCLCA2-transfected HEK-293 cells exposed to 2 mM Ca²⁺ in the pipette was absent from vector alone transfected cells (Fig. 7) (see also Refs. 9, 11, 39). This current was sensitive to DIDS (300 μM), DTT (2 mM), niflumic acid (NFA; 100 μM), and tamoxifen (10 μM) (Fig. 8). The average current recorded at +100 mV was 9.60 ± 2.87 pA/pF and was reduced to 0.15 ± 1.60 (SE) pA/pF (*n* = 5) in the presence of DIDS. Exposure to DTT reduced the mean current from 9.70 ± 6.42 to 1.96 ± 2.09 pA/pF (*n* = 6). Similarly, both NFA and tamoxifen reduced the current from a mean of 6.24 ± 4.75 to

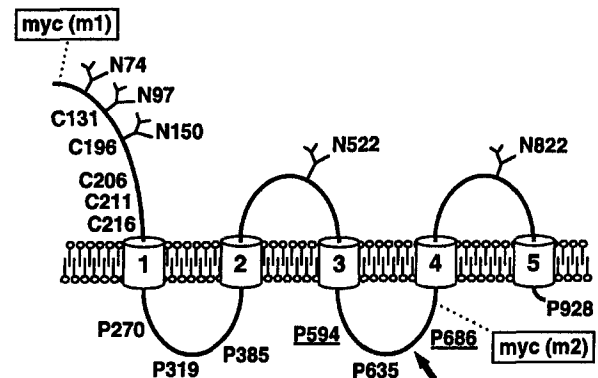


Fig. 5. Proposed transmembrane topology of hCLCA2 with transmembrane domains numbered 1-5. Dashed lines, locations of c-Myc tag in constructs m1 and m2. Sites of asparagine-linked glycosylation (Nx) are indicated by treelike drawing. Cx, cysteine residues conserved among all known CLCA homologs; Px, consensus sites for phosphorylation by protein kinase C, with sites conserved among all known homologs underlined; arrow, conserved consensus site for monobasic proteolytic cleavage.

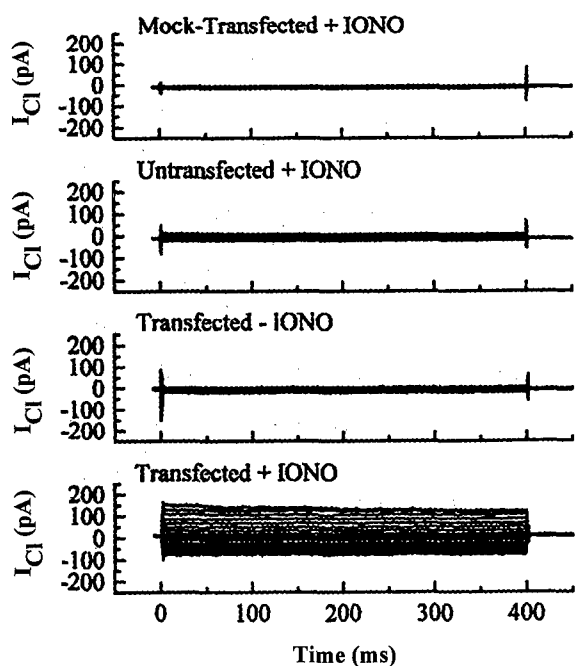


Fig. 6. Representative data collected from individual cells illustrating Cl^- current (I_{Cl}) expression in hCLCA2-transfected HEK-293 cells. In presence of low (25 nM) internal Ca^{2+} and high (2 mM) external Ca^{2+} , neither untransfected nor mock-transfected [green fluorescent protein reporter vector (EGFP) alone] HEK-293 cells showed significant current expression following exposure to ionomycin (IONO). In contrast, in hCLCA2-transfected cells, ionomycin exposure resulted in appearance of an outwardly rectified I_{Cl} .

0.64 ± 0.96 pA/pF ($n = 6$) and from 12.05 ± 3.85 to 1.02 ± 1.68 pA/pF ($n = 5$), respectively (Fig. 9). In contrast, no significant current was recorded from cells that were either untransfected or transfected with the EGFP vector alone. In the case of untransfected cells, the average current recorded in the presence of 2 mM Ca^{2+} in the pipette was 1.57 ± 0.72 pA/pF ($n = 8$), whereas, in mock-transfected cells, the current in the presence of Ca^{2+} was 0.97 ± 0.39 pA/pF ($n = 10$). When the pipette solution contained low Ca^{2+} (~25 nM) with 2 mM Ca^{2+} in the bath, perfusion of the Ca^{2+} ionophore ionomycin through the bath also activated the current (Figs. 6 and 9). Under these conditions, average currents in vector alone transfected and untransfected cells in the presence of ionomycin were 1.52 ± 1.83 ($n = 5$) and 0.22 ± 1.02 pA/pF ($n = 8$), respectively. In hCLCA2-transfected cells, addition of ionomycin increased the current from 1.7 ± 1.04 to 10.77 ± 3.8 pA/pF ($n = 7$, $P < 0.001$). These results suggest that expression of hCLCA2 in HEK-293 cells is associated with the appearance of a Ca^{2+} -sensitive Cl^- conductance.

DISCUSSION

A novel family of Ca^{2+} -activated Cl^- channels has recently been introduced by our laboratories (6, 8, 9, 11, 12). The family members cloned thus far are the bovine Lu-ECAM-1 (8, 40), the bovine Ca^{2+} -sensitive Cl^- channel (CaCC or bCLCA1) (6), the murine mCLCA1 (9), and a first human homolog, hCLCA1, which is exclu-

sively expressed in the intestine (11). Here we have described a second human family member that is expressed in human lung, trachea, and mammary gland. hCLCA2 shares many of the structural and functional peculiarities of its homologs. For example, the sizes and extent of glycosylation of the primary in vitro translation products of CLCA homologs are conserved within the family. In mammalian cells, the hCLCA2 primary translation product was cleaved into 86-kDa amino-terminal and 34-kDa carboxy-terminal polypeptides that are both associated with the outer cell surface. The corresponding cleavage products are 90 and 38 kDa for Lu-ECAM-1 (8), 90 and 37–41 kDa for hCLCA1 (11), and 90 and 32–38 kDa for mCLCA1 (9). It is unclear whether there are any structural or functional relationships between the larger amino-terminal and the smaller carboxy-terminal polypeptides of the CLCA homologs, although studies with amino- and carboxy-terminal-truncated constructs of bCLCA1 have suggested that the carboxy-terminal cleavage product is dispensable for channel function (15). Also conserved among all homologs are a pattern of amino-terminal, extracellular cysteine residues, a consensus recognition site for monobasic proteolytic cleavage that is consistent with the sizes of the two cleavage products, and consensus sites for phosphorylation by PKC, although their respective functional significance remains to be established.

Detailed biochemical analyses on the structure of hCLCA2 revealed a five-transmembrane topology with

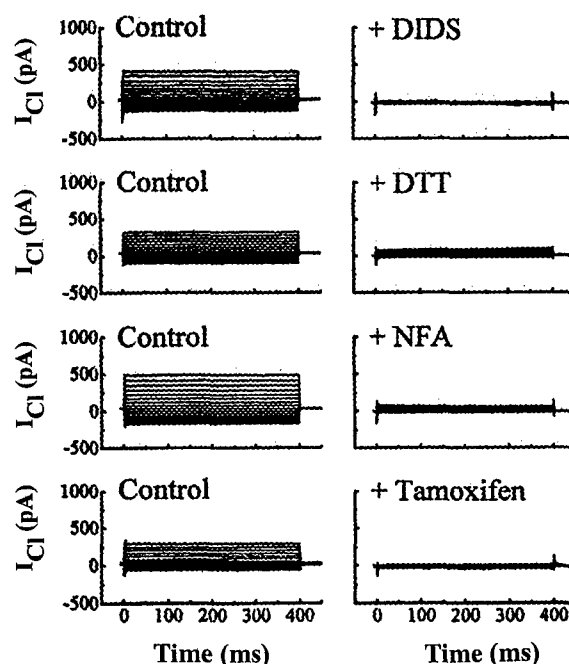


Fig. 7. Attenuation of hCLCA2 current expression by I_{Cl} inhibitors. In presence of 2 mM intracellular (pipette) and extracellular Ca^{2+} (bath), hCLCA2-transfected HEK-293 cells consistently expressed Cl^- currents with a maximum amplitude between 300 and 500 pA. Subsequent exposure to 300 mM DIDS, 2 mM dithiothreitol (DTT), 100 mM niflumic acid (NFA), or 10 mM tamoxifen resulted in near-complete inhibition of expressed current. Data are taken from individual cells.

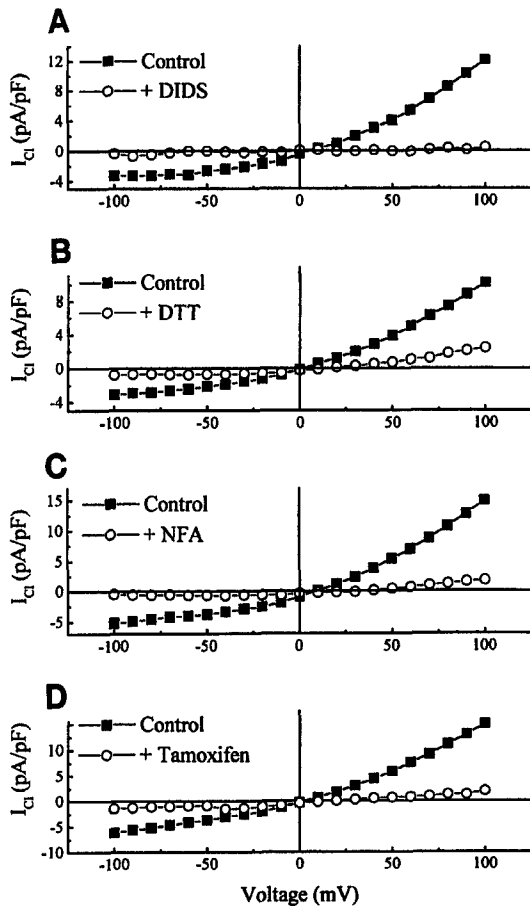


Fig. 8. Current-voltage relationship of hCLCA2 expressed in HEK-293 cells. Representative data collected from individual cells showing effect of inhibitors on whole cell currents in presence of 2 mM intracellular Ca^{2+} . Currents recorded from untransfected or EGFP alone transfected cells were negligible (see text). *A*: current expressed in hCLCA2-transfected cells displayed slight outward rectification with maximal activation of 12.06 pA/pF measured at +100 mV (■). Subsequent perfusion with 300 μ M DIDS resulted in inhibition of the current to 0.66 pA/pF (○). *B–D*: as above, using inhibitors DTT (2 mM) yielding 10.12 pA/pF (■) and 2.41 pA/pF (○), NFA (100 μ M, *C*) yielding 14.98 pA/pF (■) and 1.78 pA/pF (○), and tamoxifen (10 μ M, *D*) yielding 14.95 pA/pF (■) and 1.96 pA/pF (○).

three transmembrane domains within the 86-kDa amino-terminal and two within the 34-kDa carboxy-terminal cleavage products. This result is at variance with the models proposed for earlier cloned CLCA homologs, where, based on the much less reliable hydrophobicity analyses alone, four transmembrane regions have been suggested, all located within the larger amino-terminal cleavage product (6, 8, 9, 11). A consequence of this difference is the intracellular location of the predicted cleavage site between the two hCLCA2 subunits and extracellular locations for the proposed models for Lu-ECAM-1, mCLCA1, and hCLCA1. Therefore, the data on the CLCA homologs other than hCLCA2 need to be reevaluated, and analogous biochemical studies will have to be performed for each family member. Given similar functional characteristics among CLCA homologs, it is likely that the established hCLCA2 transmembrane topology will serve as the prototype for all members of this channel family.

Measurements on the Ca^{2+} -activated Cl^- conductance of hCLCA2 were performed in transfected HEK-293 cells. This cell line was chosen because it is devoid of any intrinsic Ca^{2+} -activated Cl^- conductance (41). Consistent with previous findings on CLCA homologs, the Ca^{2+} ionophore ionomycin elicited an increase in whole cell current in hCLCA2-expressing HEK-293 cells. This current was sensitive to standard inhibitors of Cl^- channels, such as DIDS, NFA, and tamoxifen. Although Ca^{2+} was present in the bath at unphysiological concentrations (2 mM), recent evidence suggests that ionomycin may release Ca^{2+} from the endoplasmic reticulum store exclusively, in which case its concentration only increases in the range of 200–500 nM (34). The data presented here do not unequivocally prove that hCLCA2 forms an anion channel itself but would also be consistent with a role of hCLCA2 as a regulator of an as-yet-unidentified, endogenous channel that by itself is not sensitive to Ca^{2+} . However, it has been shown that the closely related bovine tracheal bCLCA1 forms a genuine channel protein when reconstituted into planar lipid bilayers (16, 24). Under the conditions used in the present study, we did not observe any time dependence of activation of the Ca^{2+} -sensitive current. Although time-dependent activation of Ca^{2+} -sensitive Cl^- currents has been previously reported in epithelial cells (2, 37), the lack of such a characteristic may reflect the use of a heterologous expression system and the loss of associated proteins that confer this property (17). Alternatively, hCLCA2 may not underlie the time-dependent Ca^{2+} -sensitive current recorded from native airway cells, even though it is expressed in that tissue. The observation that the hCLCA2-associated current is also sensitive to the anti-estrogen tamoxifen is also consistent with a role for the expressed protein as an

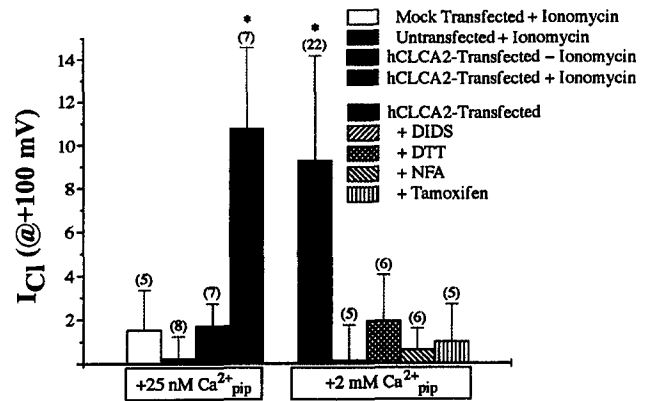


Fig. 9. Summary of effects of ionomycin and inhibitors on hCLCA2 current expression recorded at +100 mV. In presence of low cytosolic free Ca^{2+} (~25 nM), exposure of EGFP alone transfected and untransfected HEK-293 cells in presence of ionomycin yielded currents of 1.52 ± 1.83 ($n = 5$) and 0.22 ± 1.02 (SE) pA/pF ($n = 8$), respectively. Exposure of hCLCA2-transfected cells to ionomycin resulted in an increase in current from 1.69 ± 1.04 to 10.77 ± 3.8 pA/pF ($n = 7$; $*P < 0.001$). When internally perfused with solutions containing 2 mM Ca^{2+} , transfected cells exhibited a maximal current of 9.27 ± 4.91 pA/pF ($n = 22$; $*P < 0.001$). Exposure to DIDS (300 μ M), DTT (2 mM), NFA (100 μ M), or tamoxifen (10 μ M) inhibited the maximally activated currents to 0.152 ± 1.6 , 1.95 ± 2.09 , 0.64 ± 0.96 , or 1.02 ± 1.68 pA/pF, respectively.

anion channel. Several other anion channels, notably a volume-regulated channel described in Ehrlich ascites tumor cells (22), a Ca^{2+} -activated Cl^- current identified in arterial endothelial cells (21), and a member of the ClC family of Cl^- channels (39), were also shown to be sensitive to this compound. Considering the expression of hCLCA2 in human breast epithelium, it remains to be established whether its sensitivity to tamoxifen plays any role in the effectiveness of this drug against breast cancer.

The function of hCLCA2 as a mediator of a Ca^{2+} -activated Cl^- current and its expression in human lung and trachea warrant future investigations aimed at its potential involvement in the complex ion-secretory disorder of cystic fibrosis. Especially intriguing is the question whether it may form a viable alternate Cl^- channel that could be exploited for pharmacological targeting to circumvent the defect of the CFTR Cl^- channel. Studies in other systems, including animal models of cystic fibrosis, have shown that a Ca^{2+} -sensitive Cl^- conductance is present in cystic fibrosis cells and may even be upregulated. This observation is particularly relevant in the cystic fibrosis knockout mouse model, where expression of an as-yet-unidentified Ca^{2+} - and DIDS-sensitive Cl^- conductance is thought to rescue the cystic fibrosis mouse from significant airway disease (10, 27, 36). In the same CFTR (-/-) mouse, lethal intestinal pathology is associated with absence of a Ca^{2+} -activated pathway for Cl^- secretion, whereas expression of a Ca^{2+} -sensitive Cl^- conductance in the murine intestine is thought to compensate for the lack of CFTR function and rescue the intestinal phenotype (4, 36). However, to what extent the Ca^{2+} -sensitive Cl^- conductance may substitute for the defective CFTR in human cystic fibrosis is unclear, especially since data obtained in CFTR (-/-) mice may not be readily extrapolated to human cystic fibrosis due to their significantly different cystic fibrosis phenotypes (3, 4, 27, 30). A future challenge will be to establish whether differences in tissue-specific channels between species contribute to the differences observed between the phenotypes of cystic fibrosis patients and murine CFTR knockouts.

We thank Dr. Dale Benos for his assistance in the Cl^- conductance studies of hCLCA2 and Dr. Benos and Dr. Randy Elble for their constructive discussions. Heather Archibald is commended for excellent technical assistance.

This work was supported by National Institutes of Health Grants CA-47668 and CA-71626 (B. U. Pauli), DK-53090 (C. M. Fuller and D. Benos), and 5T32HL-07703-08 (K. D. Schreur), funds from the Cystic Fibrosis Foundation (C. M. Fuller), and a fellowship from the German Research Council (A. D. Gruber).

Address for reprint requests and other correspondence: B. U. Pauli, Cancer Biology Laboratories, Dept. of Molecular Medicine, Cornell Univ. College of Veterinary Medicine, Ithaca, NY 14853-6401 (E-mail: bup1@cornell.edu).

Received 10 December 1998; accepted in final form 4 March 1999.

REFERENCES

- Anderson, M. P., and M. J. Welsh. Calcium and cyclic AMP activate different chloride channels in the apical membrane of normal and cystic fibrosis epithelia. *Proc. Natl. Acad. Sci. USA* 88: 6003-6007, 1991.
- Arreola, J., J. E. Melvin, and T. Begebenisch. Inhibition of Ca^{2+} -dependent Cl^- channels from secretory epithelial cells by low internal pH. *J. Membr. Biol.* 147: 95-104, 1995.
- Clarke, L. L., B. R. Grubb, S. E. Gabriel, O. Smithies, B. H. Koller, and R. C. Boucher. Defective epithelial chloride transport in a gene-targeted mouse model of cystic fibrosis. *Science* 257: 1125-1128, 1992.
- Clarke, L. L., B. R. Grubb, J. R. Yankaskas, C. U. Cotton, A. McKenzie, and R. C. Boucher. Relationship of a non-cystic fibrosis transmembrane conductance regulator-mediated chloride conductance to organ-level disease in Cfr (-/-) mice. *Proc. Natl. Acad. Sci. USA* 91: 479-483, 1994.
- Cravchik, A., and A. A. Matus. A novel strategy for the immunological tagging of cDNA constructs. *Gene* 137: 139-143, 1993.
- Cunningham, S. A., M. S. Awayda, J. K. Bubien, I. I. Ismailov, M. P. Arrate, B. K. Berdiev, D. J. Benos, and C. M. Fuller. Cloning of an epithelial chloride channel from bovine trachea. *J. Biol. Chem.* 270: 31016-31026, 1995.
- Devi, L. Consensus sequence for processing of polypeptide precursors at monobasic sites. *FEBS Lett.* 280: 189-194, 1991.
- Elble, R., J. Widom, A. D. Gruber, M. Abdel-Ghany, R. Levine, A. Goodwin, H.-C. Cheng, and B. U. Pauli. Cloning and characterization of lung-endothelial cell adhesion molecule-1 suggest it is an endothelial chloride channel. *J. Biol. Chem.* 272: 27853-27861, 1997.
- Gandhi, R., R. C. Elble, A. D. Gruber, H.-L. Ji, S. M. Copeland, C. M. Fuller, and B. U. Pauli. Molecular and functional characterization of a calcium-sensitive chloride channel from mouse lung. *J. Biol. Chem.* 273: 32096-32101, 1998.
- Grubb, B. R., R. N. Vick, and R. C. Boucher. Hyperabsorption of Na^+ and raised Ca^{2+} -mediated Cl^- secretion in nasal epithelia of CF mice. *Am. J. Physiol.* 266 (Cell Physiol. 35): C1479-C1483, 1994.
- Gruber, A. D., R. C. Elble, H.-L. Ji, K. D. Schreur, C. M. Fuller, and B. U. Pauli. Genomic cloning, molecular characterization, and functional analysis of human CLCA1, the first human member of the family of Ca^{2+} -activated Cl^- channels. *Genomics* 54: 200-214, 1998.
- Gruber, A. D., R. Gandhi, and B. U. Pauli. The murine calcium-sensitive chloride channel (mCaCC) is widely expressed in secretory epithelia and other select tissues. *Histochem. Cell Biol.* 110: 43-49, 1998.
- Gruber, A. D., and R. A. Levine. In situ assessment of mRNA accessibility in heterogeneous tissue samples using elongation factor 1 α (EF-1 α). *Histochem. Cell Biol.* 107: 411-416, 1997.
- Jentsch, T. J., W. Gunther, M. Pusch, and Schwappach. Properties of voltage-gated chloride channels of the ClC gene family. *J. Physiol. (Lond.)* 482: 19S-25S, 1995.
- Ji, H.-L., M. D. DuVall, H. K. Patton, C. L. Satterfield, C. M. Fuller, and D. J. Benos. Functional expression of a truncated Ca^{2+} -activated Cl^- channel and activation by phorbol ester. *Am. J. Physiol.* 274 (Cell Physiol. 43): C455-C464, 1998.
- Jovov, B., I. Ismailov, and D. J. Benos. Interaction between cystic fibrosis transmembrane conductance regulator and outwardly rectified chloride channels. *J. Biol. Chem.* 270: 29194-29200, 1995.
- Jovov, B., V. G. Shlyonsky, B. K. Berdiev, I. I. Ismailov, and D. J. Benos. Purification and reconstitution of an outwardly rectified Cl^- channel from tracheal epithelia. *Am. J. Physiol.* 275 (Cell Physiol. 44): C449-C458, 1998.
- Knowles, M. R., L. L. Clarke, and R. C. Boucher. Activation by extracellular nucleotides of chloride secretion in the airway epithelia of patients with cystic fibrosis. *N. Engl. J. Med.* 325: 533-538, 1991.
- Knowles, M. R., J. Gatzky, and R. C. Boucher. Relative ion permeability of normal and cystic fibrosis nasal epithelium. *J. Clin. Invest.* 71: 1410-1417, 1983.
- Mason, S. J., A. M. Paradiso, and R. C. Boucher. Regulation of transepithelial ion transport and intracellular calcium by extracellular ATP in human normal and cystic fibrosis airway epithelium. *Br. J. Pharmacol.* 103: 1649-1656, 1991.
- Nilius, B., J. Prenen, G. Szucs, L. Wei, F. Tanzi, T. Voets, and G. Droogmans. Calcium-activated chloride channels in bovine

- pulmonary artery endothelial cells. *J. Physiol. (Lond.)* 498: 381-396, 1997.
22. Pedersen, S. F., J. Prenen, G. Droogmans, E. K. Hoffman, and B. Nilius. Separate swelling and Ca^{2+} -activated anion currents in Ehrlich ascites tumor cells. *J. Membr. Biol.* 163: 97-110, 1998.
 23. Quinton, P. M. Chloride impermeability in cystic fibrosis. *Nature* 301: 421-422, 1983.
 24. Ran, S., and D. J. Benos. Immunopurification and structural analysis of a putative epithelial Cl^- channel protein isolated from bovine trachea. *J. Biol. Chem.* 267: 3618-3625, 1992.
 25. Riordan, J. R., J. M. Rommens, B. Kerem, N. Alon, R. Rozmahel, Z. Grzelczak, J. Zielenski, S. Lok, N. Plavsic, J.-L. Chou, M. L. Drumm, M. C. Iannuzzi, F. S. Collins, and L.-C. Tsui. Identification of the cystic fibrosis gene: cloning and characterization of complementary DNA. *Science* 245: 1066-1073, 1989.
 26. Rommens, J. M., M. C. Iannuzzi, B. Kerem, M. L. Drumm, G. Melmer, M. Dean, R. Rozmahel, J. L. Cole, D. Kennedy, N. Hidaka, N. Zsiga, M. Buchwald, J. R. Riordan, L.-C. Tsui, and F. S. Collins. Identification of the cystic fibrosis gene: chromosome walking and jumping. *Science* 245: 1059-1065, 1989.
 27. Rozmahel, R., M. Wilschanski, A. Matin, S. Plyte, M. Oliver, W. Auerbach, A. Moore, J. Forstner, P. Durie, J. Nadeau, C. Bear, and L.-C. Tsui. Modulation of disease severity in cystic fibrosis transmembrane conductance regulator deficient mice by a secondary genetic factor. *Nat. Genet.* 12: 280-287, 1996.
 28. Schmidt-Rose, T., and T. J. Jentsch. Transmembrane topology of a CLC chloride channel. *Proc. Natl. Acad. Sci. USA* 94: 7633-7638, 1997.
 29. Schwiebert, E. M., M. E. Egan, T.-H. Hwang, S. B. Fulmer, S. S. Allen, G. R. Cutting, and W. B. Guggino. CFTR regulates outwardly rectifying chloride channels through an autocrine mechanism involving ATP. *Cell* 81: 1063-1073, 1995.
 30. Snouwaert, J. N., K. K. Brigman, A. M. Latour, N. N. Malouf, R. C. Boucher, O. Smithies, and B. H. Koller. An animal model for cystic fibrosis made by gene targeting. *Science* 257: 1083-1088, 1992.
 31. Stutts, M. J., C. M. Canessa, J. C. Olsen, M. Hamrick, J. A. Cohn, B. C. Rossier, and R. C. Boucher. CFTR as a cAMP-dependent regulator of Na^+ channels. *Science* 269: 847-850, 1995.
 32. Von Heijne, G. A new method for predicting signal sequence cleavage sites. *Nucleic Acids Res.* 14: 4683-4690, 1986.
 33. Wagner, J. A., A. L. Cozens, H. Schulman, D. C. Cotton, A. McKenzie, and R. C. Boucher. Activation of chloride channels in normal and cystic fibrosis airway epithelial cells by multifunctional calcium/calmodulin dependent protein kinase. *Nature* 349: 793-796, 1991.
 34. Waldron, R. T., A. D. Short, and D. L. Gill. Store-operated Ca^{2+} entry and coupling of Ca^{2+} pool depletion in thapsigargin-resistant cells. *J. Biol. Chem.* 272: 6440-6447, 1997.
 35. Willumsen, N. J., and R. C. Boucher. Activation of an apical Cl^- conductance by Ca^{2+} ionophores in cystic fibrosis airway epithelia. *Am. J. Physiol.* 256 (*Cell Physiol.* 25): C226-C235, 1989.
 36. Wilschanski, M. A., R. Rozmahel, S. Beharry, G. Kent, C. Lui, L.-C. Tsui, P. Durie, and C. E. Bear. In vivo measurements of ion transport in long-living CF mice. *Biochem. Biophys. Res. Commun.* 219: 753-759, 1996.
 37. Winpenny, J. P., A. Harris, M. A. Hollingsworth, B. E. Argent, and M. A. Gray. Calcium-activated chloride conductance in a pancreatic adenocarcinoma cell line of ductal origin (HPAF) and in freshly isolated human pancreatic duct cells. *Pflügers Arch.* 435: 796-803, 1998.
 38. Wo, Z. G., and R. E. Oswald. Transmembrane topology of two kinase receptor subunits revealed by N-glycosylation. *Proc. Natl. Acad. Sci. USA* 91: 7154-7158, 1994.
 39. Yamazaki, J., D. Duan, R. Janiak, K. Kuenzli, B. Horowitz, and J. R. Hume. Functional and molecular expression of volume-regulated chloride channels in canine vascular smooth muscle cells. *J. Physiol. (Lond.)* 507: 729-736, 1998.
 40. Zhu, D. Z., C. F. Cheng, and B. U. Pauli. Mediation of lung metastasis of murine melanomas by a lung-specific endothelial cell adhesion molecule. *Proc. Natl. Acad. Sci. USA* 88: 9568-9572, 1991.
 41. Zhu, G., Y. Zhang, H. Xu, and C. Jiang. Identification of endogenous outward currents in the human embryonic kidney (HEK 293) cell line. *J. Neurosci. Methods* 81: 73-83, 1998.

The Breast Cancer β_4 Integrin and Endothelial Human CLCA2 Mediate Lung Metastasis*

Received for publication, January 18, 2001, and in revised form, April 19, 2001
Published, JBC Papers in Press, April 24, 2001, DOI 10.1074/jbc.M100478200

Mossaad Abdel-Ghany, Hung-Chi Cheng, Randolph C. Elble, and Bendicht U. Pauli‡

From the Cancer Biology Laboratories, Department of Molecular Medicine, Cornell University College of Veterinary Medicine, Ithaca, New York 14853

Adhesion of blood-borne cancer cells to the endothelium is a critical determinant of organ-specific metastasis. Here we show that colonization of the lungs by human breast cancer cells is correlated with cell surface expression of the $\alpha_6\beta_4$ integrin and adhesion to human CLCA2 (hCLCA2), a Ca^{2+} -sensitive chloride channel protein that is expressed on the endothelial cell luminal surface of pulmonary arteries, arterioles, and venules. Tumor cell adhesion to endothelial hCLCA2 is mediated by the β_4 integrin, establishing for the first time a cell-cell adhesion property for this integrin that involves an entirely new adhesion partner. This adhesion is augmented by an increased surface expression of the $\alpha_6\beta_4$ integrin in breast cancer cells selected *in vivo* for enhanced lung colonization but abolished by the specific cleavage of the β_4 integrin with matrilysin. β_4 integrin/hCLCA2 adhesion-blocking antibodies directed against either of the two interacting adhesion molecules inhibit lung colonization, while overexpression of the β_4 integrin in a model murine tumor cell line of modest lung colonization potential significantly increases the lung metastatic performance. Our data clearly show that the β_4 /hCLCA2 adhesion is critical for lung metastasis, yet expression of the β_4 integrin in many benign breast tumors shows that this integrin is insufficient to bestow metastatic competence on cells that lack invasiveness and other established properties of metastatic cells.

Colonization of secondary organs by blood-borne cancer cells marks the final, usually fatal stage in a long, multistep cascade of tumor progression that is propelled by an array of acquired, cumulative, genetic abnormalities and promoting tissue micro-environmental cues (1–5). Increasing evidence suggests that tumor cell targeting of preferred, secondary organs for metastasis is mediated by distinct endothelial cell adhesion molecules (6–8). These molecules are expressed constitutively (organ-specifically) on the endothelial cell luminal surface of select vascular compartments (*e.g.* capillaries, arterioles, and/or venules) (7). By binding blood-borne cancer cells at high affinity, these molecules mediate vascular arrest of tumor cells under hydrodynamic conditions (6–9) and, as shown recently, promote intravascular growth to form tumor colonies at these

secondary target sites (10, 11). Using a unique large vessel endothelial cell system, in which an organ-specific vascular phenotype can be induced by growing “neutral” bovine aortic endothelial cells on matrix extracts of that organ (12), a lung-specific endothelial cell adhesion molecule, termed Lu-ECAM-1 (lung-endothelial cell adhesion molecule-1) was isolated, purified, and cloned by our laboratory (13–15). Lu-ECAM-1 is the prototype of a newly discovered mammalian family of proteins (termed CLCAs, for Cl^- channel proteins, Ca^{2+} -activated) (13), which, similar to the cystic fibrosis transmembrane conductance regulator (16, 17), serve the dual function of mediating chloride conductance and cell-cell adhesion (16–18). Lu-ECAM-1 protein, like all other members of the CLCA family, is synthesized as an ~125-kDa precursor protein that, upon membrane incorporation, is rapidly processed into N-terminal 90-kDa and C-terminal 35-kDa components (15, 18). The 90-kDa polypeptide is responsible for the adhesion qualities of CLCAs, promoting the Ca^{2+} -dependent adhesion of a variety of lung metastatic cancer cells but not cancer cells that metastasize to other organ sites (12–15).

In this report, hCLCA2¹ cloned from a lung cDNA library (19) is identified as the human counterpart of Lu-ECAM-1. We show that hCLCA2 is expressed by endothelia from different lung vascular compartments and that lung colonization of established human breast cancer cell lines is dependent upon the tumor cells' ability to interact with hCLCA2. Breast cancer cell adhesion to hCLCA2 is mediated by the β_4 integrin, which is prominently expressed in breast cancer cells that are able to colonize the lungs upon tail vein injection of nude mice (20). Cell-to-cell adhesion assays, adhesion-blocking assays with antibodies generated against either of the two interacting molecules, and overexpression of β_4 in a murine model tumor cell line are used to confirm involvement of the β_4 integrin/hCLCA2 adhesion mechanism in lung metastasis. Together, our data confirm that the $\alpha_6\beta_4$ integrin is a lung metastasis-associated gene (21) and establish for the first time a cell-to-cell adhesion property for the β_4 integrin that involves an entirely new integrin adhesion partner.

EXPERIMENTAL PROCEDURES

Antibodies and Reagents—Anti-Lu-ECAM-1 mAb 6D3 was produced in BALB/c mice (22) and selected for adhesion blocking of B16-F10 melanoma cells to Lu-ECAM-1-expressing bovine aortic endothelial cells (13, 14). Rabbit polyclonal antibodies (pAbs) 4 and 18 were gener-

* This work was supported by NCI, National Institutes of Health, Public Health Service Grants CA47668 and CA71626 (to B. U. P.). The costs of publication of this article were defrayed in part by the payment of page charges. This article must therefore be hereby marked “advertisement” in accordance with 18 U.S.C. Section 1734 solely to indicate this fact.

‡ To whom correspondence should be addressed: Cancer Biology Laboratories, Dept. of Molecular Medicine, Cornell University College of Veterinary Medicine, Ithaca, New York 14853. Tel.: 607-253-3343; Fax: 607-253-3708; E-mail: bup1@cornell.edu.

¹ The abbreviations used are: hCLCA2, human CLCA2; mCLCA1, mouse CLCA1; mAb, monoclonal antibody; pAb, polyclonal antibody; HMVEC-L, human lung microvascular endothelial cells; HAEC, human aortic endothelial cells; HUVEC, human umbilical vein endothelial cells; HEK, human embryonic kidney; RT, reverse transcriptase; PCR, polymerase chain reaction; PAGE, polyacrylamide gel electrophoresis; BSA, bovine serum albumin; HRP, horseradish peroxidase; FACS, fluorescence-activated cell sorting; DMEM, Dulbecco's modified Eagle's medium.

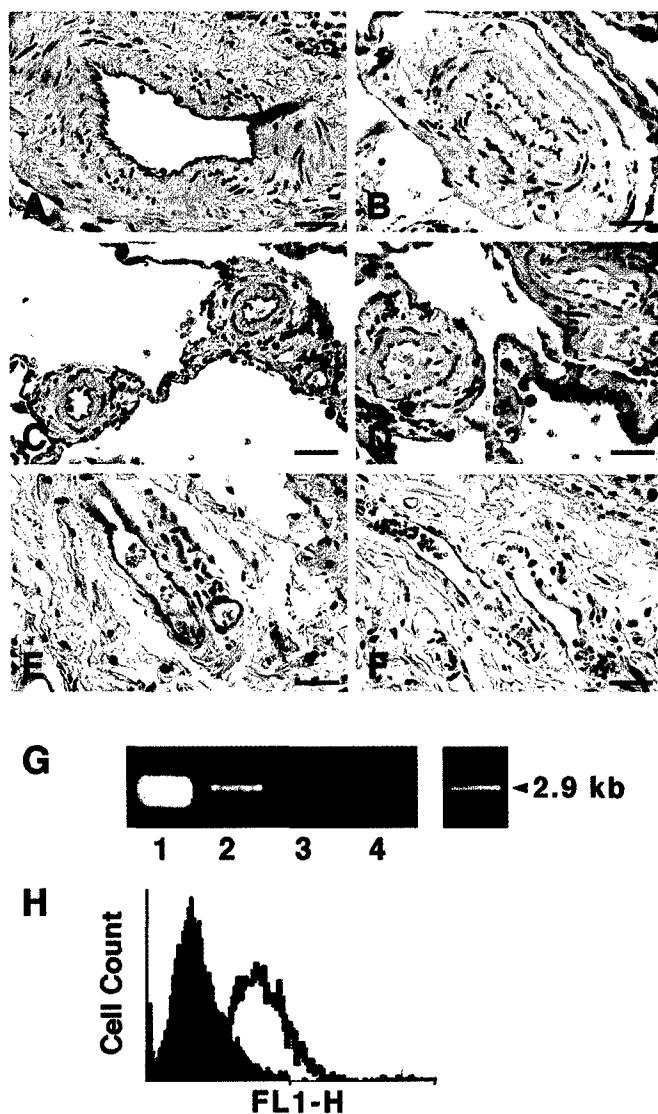


FIG. 1. Endothelial cell expression of hCLCA2. A–F, sections (2 μ m thick) from paraffin-embedded, formaldehyde-fixed lung tissue blocks were stained with rabbit anti-hCLCA2 pAb 4 at a dilution of 1:100 (A, C, and E) or rabbit preimmune IgG (B, D, and F). Bound antibody was detected by HRP-conjugated goat anti-rabbit IgG antibodies and diaminobenzidine as substrate. A positive staining reaction is observed in small arteries (A), arterioles (C), and venules of interlobular septa (E). Comparable vessels stained with preimmune serum are negative (B, D, F). Bar, 100 μ m. G and H, expression of hCLCA2 in cultured endothelial cells is shown by RT-PCR amplification of an 800-base pair hCLCA2 product from total RNA of HMVEC-L (lane 1), HAEC (lane 2), and HUVEC (lane 3) but not HEK293 (lane 4) (see “Experimental Procedures”) and of the full-length 2.9-kilobase pair hCLCA2 open reading frame from HMVEC-L RNA (G) and by FACS analysis of HMVEC-L stained with rabbit anti-hCLCA2 pAb 4 (open histogram) or rabbit preimmune IgG (closed histogram) and fluorescein isothiocyanate-conjugated goat anti-rabbit IgG (H).

ated against the hCLCA2 peptides KANNNSKIQESYKENV (amino acids 94–111) and ESTGENVKPHHQLKNTVTVD (amino acids 498–517), respectively. Antibodies against the β_4 integrin ectodomain included mouse mAb 3E1 (Life Technologies, Inc.), rabbit pAb H101 (Santa Cruz Biotechnology, Inc., Santa Cruz, CA), and rabbit pAb 81435 directed against TA3/HA mouse mammary carcinoma cells (Dr. E. Roos, The Netherlands Cancer Institute, Amsterdam) (23). Rat anti-human α_6 integrin mAb GoH3 was from PharMingen (San Diego, CA), mouse anti-human β_1 mAb 2253 from Chemicon (Temecula, CA), and mouse anti-human Myc mAb 9E10 and anti-phosphotyrosine mAb from Calbiochem. Human placental and murine EHS laminins as well as all other reagents were from Sigma.

Cell Cultures—Human breast cancer cell lines MDA-MB-231, -435, -468, and -453 and MCF7 were from the ATCC (Manassas, VA). MDA-

MB-435L2 was from Dr. J. E. Price (The University of Texas M.D. Anderson Cancer Center, Houston, TX) (20), and MDA-MB-435 transfected with wild type human β_4 integrin or tailless β_4 integrin ($\beta_4\Delta$ Cyt) were from Dr. A. M. Mercurio (Beth Israel Deaconess Medical Center and Harvard Medical School, Boston, MA) (24). Human lung microvascular endothelial cells (HMVEC-L) and human aortic endothelial cells (HAEC) were from Clonetics (San Diego, CA). Human umbilical vein endothelial cells (HUVEC), human embryonic kidney 293 cells (HEK293), and Kirsten Ras-transformed Balb/3T3 (K-Balb/3T3) cells were from the ATCC. HMVEC-L were grown in EGM-2-MV BulletKit medium (Clonetics), and all others were grown in Dulbecco’s modified Eagle’s medium (DMEM) supplemented with 10% heat-inactivated fetal bovine serum (Life Technologies).

RT-PCR Analyses—Total RNA isolated from HMVEC-L, HAEC, and HUVEC was reverse-transcribed, and an 800-base pair hCLCA2 product amplified by PCR, using ttctctacaacatgacccaaaggagc and catgg-gaaagctgtgggaaag as 5’ and 3’ primers, respectively, and Taq polymerase (Life Technologies) (19). The full-length 2.9-kilobase pair open reading frame of hCLCA2 was amplified from HMVEC-L RNA, using primers corresponding to the 5’ (ttctctacaacatgacccaaaggagc) and 3’ (gacacttggatattattataataattttgttc) ends of the hCLCA2 open reading frame. Both primer sets were tested on cloned plasmid templates to ascertain that they would not recognize other CLCA homologs. RNA extracted from HEK293 cells and processed in parallel served as negative control.

Expression, Myc Tagging, Immunoprecipitation, and Purification of hCLCA2—Lung expression of hCLCA2 was analyzed by staining sections of paraffin-embedded, formaldehyde (4%) fixed tissue with rabbit anti-hCLCA2 antiserum (pAb 4) at a 1:100 dilution (13, 22). Preimmune serum used at the same dilution served as control. Myc-tagged hCLCA2 constructs were generated as described and transfected into 80% confluent HEK293 using the LipofectAMINE™ Plus protocol (Life Technologies) (19). Immunoprecipitated and immunopurified hCLCA2 were from extracts of transfected HEK293 cells (48 h after transfection), using anti-Myc mAb 9E10-conjugated goat anti-mouse IgG Dynabeads (or Protein G beads). Surface expression of hCLCA2 was confirmed by cell surface biotinylation (100 μ g/ml Biotin *N*-hydroxysuccinimide) (25). Western blot analyses were done with anti-Myc mAb 9E10 (19).

Isolation, Purification, and Phosphorylation of the β_4 Integrin Ligand of hCLCA2—The tumor cell ligand of hCLCA2 was isolated from lysates of surface-biotinylated MDA-MB-231 breast cancer cells bound to a monolayer of transiently transfected Myc-hCLCA2-HEK293 cells by co-immunoprecipitation with anti-Myc mAb 9E10. In brief, MDA-MB-231 cells (5×10^4 tumor cells/cm² of HEK293 monolayer surface) were allowed to adhere to Myc-hCLCA2-HEK293 monolayers (or control vector-transfected HEK293 monolayers) during a 20-min incubation period. After removing unbound tumor cells by washing, bound tumor cells and HEK293 cells were extracted in lysis buffer (26, 27), and extracts were subjected to immunoprecipitation with anti-Myc mAb 9E10. Immunoprecipitates were resolved by SDS-PAGE (6% polyacrylamide), blotted to nitrocellulose, and probed with streptavidin-HRP or anti- β_4 mAb 3E1 followed by HRP-conjugated secondary antibody. Alternatively, the hCLCA2 tumor cell ligand was isolated by affinity chromatography from surface-biotinylated MDA-MB-231 cells using Myc-hCLCA2-conjugated anti-Myc mAb 9E10/goat anti-mouse IgG Dynabeads. Beads were boiled in SDS-sample buffer, and proteins were resolved by SDS-PAGE and blotted to nitrocellulose. Blots were probed with streptavidin-HRP, anti- β_4 mAb 3E1, or anti-Myc mAb 9E10. Purification of β_4 was accomplished with anti- β_4 mAb 3E1-conjugated Protein G beads from lysates of MDA-MB-231 cells (10^8 cells/preparation). To further corroborate the specificity of the β_4 /hCLCA2 adhesion, MDA-MB-231 cancer cells were labeled with $H_3^{32}PO_4$ (0.5 mCi/ml) in phosphate-free DMEM for 4 h at 37 °C and then seeded onto BSA-, fibronectin-, hCLCA2-, laminin-, and poly-L-lysine-coated dishes and incubated for 20 min at 37 °C. Cell lysates were immunoprecipitated with anti- β_4 mAb 3E1, and precipitates were resolved by SDS-PAGE, treated with 1 M KOH for 2 h at 55 °C, and autoradiographed to visualize β_4 integrin tyrosine phosphorylation (28).

Gel Overlay (Far Western)— β_4 (immunopurified from MDA-MB-231), β_1 ($\alpha_5\beta_1$), and β_3 ($\alpha_3\beta_3$) (both from Chemicon) integrins were resolved by SDS-PAGE, blotted to nitrocellulose, denatured with 2.5 M guanidine, and renatured in 5% milk in Tris-buffered saline containing 0.1% Tween 20 (29). Blots were incubated with Myc-tagged hCLCA2 (overnight; 4 °C), and bound hCLCA2 was detected with anti-Myc mAb 9E10, followed by HRP-conjugated secondary antibody. Controls included blots probed with antibody alone. Positions on the gel and loading quantities of the β integrins were determined in parallel Western blots.

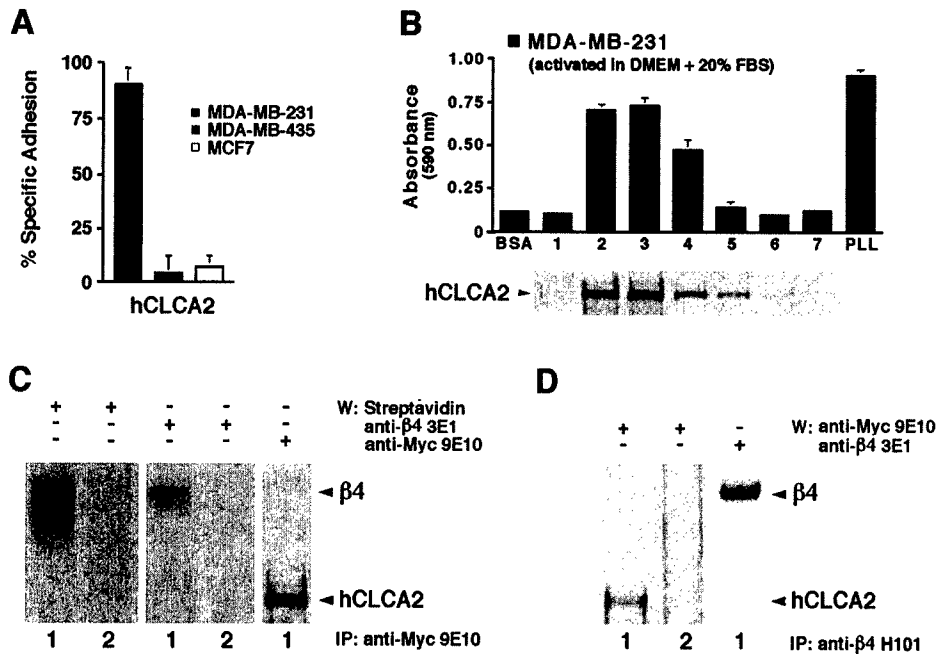


FIG. 2. The β_4 integrin mediates adhesion of breast cancer cells to endothelial hCLCA2. *A*, adhesion of MDA-MB-231, MDA-MB-435, and MCF7 human breast cancer cells to hCLCA2 was tested in microtitration plates coated with $\sim 3 \mu\text{g/ml}$ recombinant hCLCA2 (overnight; 4°C). *B*, adhesion of MDA-MB-231 cells to Myc-tagged hCLCA2 from successive elution fractions of an anti-Myc mAb 9E10-immunoaffinity column. Protein G beads conjugated with anti-Myc mAb 9E10 were incubated with extracts from HEK293 cells transfected with Myc-tagged hCLCA2 (overnight; 4°C), and bound protein was eluted with 200 mM glycine (pH 2.8) in 150 mM NaCl and 0.5% octyl- β -glucoside. Elutes were collected in 1-ml fractions in 0.1 volume of 1 M Tris (pH 11) to yield a final pH of 8.2. Each fraction was evaluated for MDA-MB-231 adhesion and protein content by Western blotting with anti-Myc mAb 9E10. Adhesion values correlate well with the amount of hCLCA2 protein in the column fraction. *C*, surface-biotinylated or untreated MDA-MB-231 cells bound to HEK293 cell monolayers transfected with Myc-hCLCA2 (*lanes 1*) or HEK293 cell monolayers transfected with vector alone (*lanes 2*) (see "Experimental Procedures") were extracted in lysis buffer containing 5 mM EGTA. Extracts were subjected to immunoprecipitation with anti-Myc mAb 9E10, and SDS-PAGE-resolved and blotted precipitates were probed with streptavidin-HRP (*left panel*), anti- β_4 mAb 3E1 (*middle panel*), or anti-Myc mAb 9E10 (*right panel*). *D*, anti- β_4 pAb H101 immunoprecipitate from extracts of MDA-MB-231 bound to Myc-tagged hCLCA2-transfected (*lanes 1*) or vector-transfected (*lane 2*) HEK293 monolayers were probed by Western blot with anti-Myc mAb 9E10 (*left panel*) or anti- β_4 mAb 3E1 (*right panel*).

Transfection of K-Balb/3T3 Cells with β_4 cDNA—Wild-type β_4 cDNA cloned into the expression vector pRC-CMV was from Dr. F. G. Giancotti. K-Balb/3T3 cells at 70% confluence were stably transfected with β_4 cDNA by electroporation and selected for G418 resistance. Controls were K-Balb/3T3 cells transfected with vector alone. Cells were used for (a) FACS to quantify β_4 surface expression (25), (b) adhesion to immunopurified mCLCA1 (14), and (c) lung colony assays (12–14).

FACS Analyses, Adhesion, and Lung Colony Assays—FACS analyses, adhesion assays, and lung colony assays were performed as previously described in detail by our laboratory (12–14, 25).

RESULTS

hCLCA2 Expression by Endothelia of the Lung Vasculature—Human CLCA2 was cloned from a human lung cDNA library, and its amino acid sequence, protein processing, transmembrane topography, and channel properties are described elsewhere (19). Northern blot hybridization and/or RT-PCR revealed epithelial expression of hCLCA2 in the mammary gland and trachea (19), while RT-PCR and immunohistochemistry demonstrated endothelial cell expression in the lungs (Fig. 1). In the latter, hCLCA2 protein was expressed selectively in endothelia of small pulmonary arteries, arterioles, and subpleural and interlobular venules (Fig. 1, A–F), while endothelia in other tissues including brain, liver, pancreas, kidney, alimentary tract, testis, ovary, adrenal gland, thyroid, and skeletal muscle were negative (data not shown). Strong hCLCA2 expression was also observed in cultured HMVEC-L lung microvascular endothelial cells, while a weak hCLCA2 expression was recorded for endothelial cells derived from human aorta (HAEC) and umbilical vein (HUVEC) (Fig. 1G). Expression of hCLCA2 protein in HMVEC-L was confirmed by FACS, using the same polyclonal antibody that had been employed in the immunohistochemical studies (Fig. 1H).

hCLCA2 Mediates Adhesion of Human Breast Cancer Cells

via the β_4 Integrin—The selective expression of hCLCA2 on endothelia of lung blood vessels, which recently were implicated with location of tumor cell arrest and early intravascular micrometastasis formation by *in situ* epifluorescence microscopy (11), suggested that hCLCA2 could serve as the human counterpart of Lu-ECAM-1 and might play a major role in lung metastasis of blood-borne human cancer cells. To test this hypothesis, we selected three human breast cancer cells with different biological behaviors for adhesion to recombinant Myc-tagged hCLCA2 immunopurified from transfected HEK293 cells. The first cell line was MDA-MB-231, which efficiently colonizes the lungs of nude mice following tumor formation from cancer cells injected into mammary fat pads (orthotopic tumor xenografts) or intravenous injection; the second cell line was MDA-MB-435, which only forms lung metastases from orthotopic tumor xenografts but not after intravenous injection; and the third cell line was MCF7, which is nonmetastatic by either of the two modalities (20). Consistent with the proposed role of hCLCA2 in lung metastasis, only MDA-MB-231 cells adhered in strong numbers to recombinant hCLCA2 (Fig. 2A). Adhesion correlated with the amount of Myc-tagged hCLCA2 protein present in elution fractions from anti-Myc mAb 9E10 immunoaffinity columns and was dependent upon serum activation of tumor cells (Fig. 2B). To identify the tumor cell molecule that served as the ligand for hCLCA2, surface-biotinylated MDA-MB-231 cancer cells were allowed to bind to confluent monolayers of Myc-tagged hCLCA2- or vector-transfected HEK293 cells, yielding tumor cell adhesion values of $\sim 75\%$ for Myc-hCLCA2-HEK293 monolayers and 25% for vector-transfected HEK293 monolayers. Myc-hCLCA2-HEK293 monolayers were extracted together with bound tumor cells, and extracts were subjected to immunoprecipitation with anti-

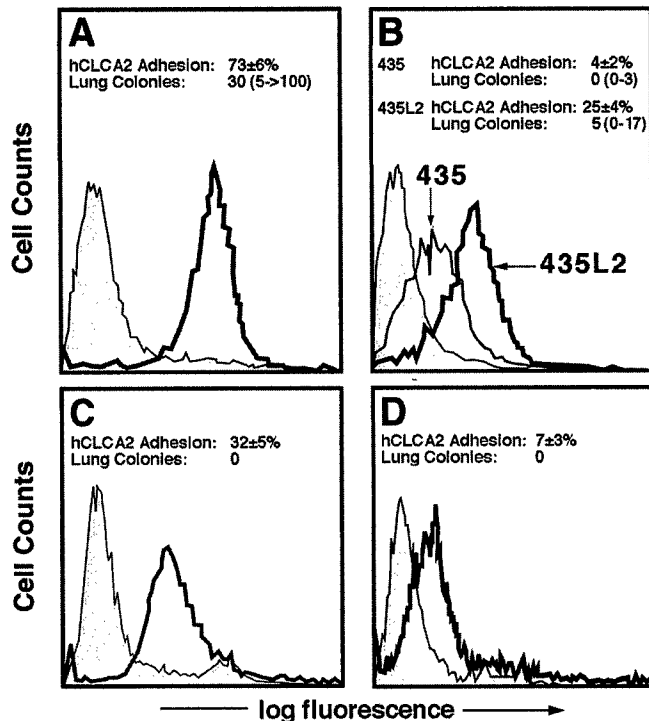


FIG. 3. The β_4 integrin expression correlates with hCLCA2 adhesion and lung colonization: FACS analyses of MDA-MB-231 (A), MDA-MB-435 (435) and MDA-MB-435L2 (435L2) (B), MDA-MB-468 (C), and MCF7 (D). Tumor cells were stained with either mouse anti- β_4 mAb 3E1 (open histogram) or mouse IgG (gray filled histogram) and fluorescein isothiocyanate-conjugated goat-anti mouse IgG secondary antibody and then subjected to FACS analyses. The percentage of tumor cell adhesion to hCLCA2-coated dishes (3 μ g/ml) and the number of lung colonies formed by each breast cancer cell line are displayed as insets.

Myc mAb 9E10. Precipitated proteins resolved by SDS-PAGE and blotted to nitrocellulose were then probed with streptavidin-HRP. A single band of molecular size 205 kDa was identified that by Western analysis with anti- β_4 mAb 3E1 was shown to be β_4 integrin (Fig. 2C). Subsequent immunoprecipitation of Myc-hCLCA2-HEK293/MDA-MB-231 cell extracts with anti- β_4 pAb H101 and Western probing of the precipitate with anti-Myc mAb 9E10 identified hCLCA2, further confirming the β_4 integrin/hCLCA2 adhesion (Fig. 2D). Controls conducted with MDA-MB-231 cancer cells bound unspecifically to vector-transfected HEK293 monolayers did not yield any precipitate. Expansion of our initial hCLCA2/tumor cell adhesion studies to MDA-MB-435L2, MDA-MB-468, and MDA-MB-453 breast cancer cell lines supported the close correlation between surface expression of the β_4 integrin, hCLCA2 adhesion, and lung colonization (Fig. 3, A-D). For example, the consistently high lung colonization potential of the MDA-MB-231 cell line correlated with high levels of β_4 integrin expression and hCLCA2 adhesion, while modest lung colonization of the MDA-MB-435L2 cell line was associated with modest β_4 expression and hCLCA2 adhesion (Fig. 3, A-D). All other breast cancer cell lines were unable to form lung colonies and, with the exception of the MDA-MB-468 cell line, expressed low or nondetectable levels of the β_4 integrin and adhered poorly to hCLCA2 (Fig. 3, A-D). In the metastatically incompetent MDA-MB-468 cell line, an intermediate level of β_4 expression correlated with a well differentiated, near normal cellular phenotype *in vitro* and slow adenomatous growth *in vivo*, implying that the MDA-MB-468 cell line represents an early stage in tumor progression.

Since isolation of the β_4 integrin-hCLCA2 complex from MDA-MB-231/Myc-hCLCA2-HEK293 extracts and hCLCA2 affinity purification of the β_4 integrin from MDA-MB-231 ex-

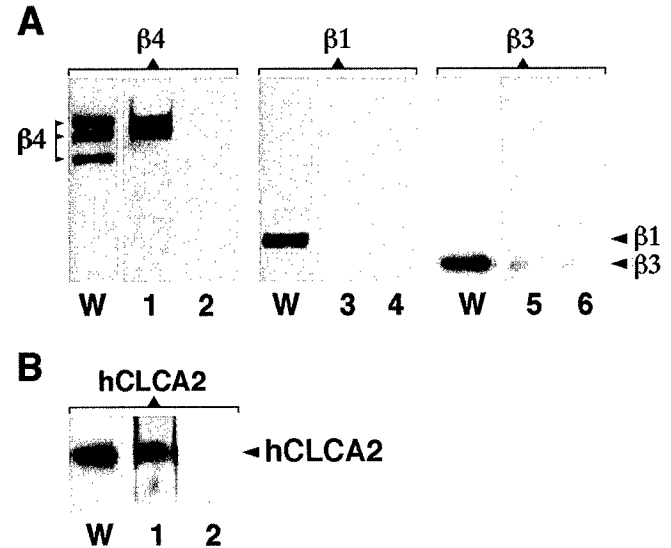


FIG. 4. Documentation of the β_4 integrin/hCLCA2 adhesion by far Western analysis. Immunopurified integrins β_4 ($\alpha_6\beta_4$), β_1 ($\alpha_5\beta_1$), and β_3 ($\alpha_6\beta_3$) (A) and hCLCA2 (B) were resolved by SDS-PAGE and blotted to nitrocellulose and then probed immediately with the respective anti- β integrin antibodies (A) or anti-Myc mAb 9E10 (B) to confirm equal protein loading (W). After successive denaturing and renaturing cycles (29), parallel blots were incubated with immunopurified Myc-hCLCA2 (lanes 1, 3, and 5) or 1% BSA (lanes 2, 4, and 6) (A) or with immunopurified β_4 integrin (lane 1) or 1% BSA (lane 2) (B) and probed with anti-Myc mAb 9E10 (A) or anti- β_4 pAb H101 (B), respectively. In A only the β_4 integrin is able to bind Myc-hCLCA2 (lane 1). Note that the β_4 used in this study appears as a triplet of 205, 180, and 150 kDa (W), since it has been extracted from MDA-MB-231 cells in lysis buffer in the absence of 5 mM EGTA (26, 27). In B, immobilized hCLCA2 strongly binds the β_4 integrin (lane 1), but not anti- β_4 antibody alone (lane 2).

tracts (data not shown) were unable to rule out participation of an unknown, intermediary molecule in the binding of hCLCA2 to β_4 integrin, the β_4 /hCLCA2 partnership was further examined by Far Western analysis. To accomplish this, adhesion receptor and ligand were first immunopurified from hCLCA2-transfected HEK293 cells and MDA-MB-231 cells, respectively, and their purity was assessed by SDS-PAGE and silver staining. After subjecting the SDS-PAGE resolved, blotted β_4 integrin to cycles of denaturing and renaturing, blots were probed with Myc-tagged hCLCA2, and hCLCA2-binding to β_4 was visualized by anti-Myc antibodies. hCLCA2 strongly and specifically bound to β_4 integrin, but not to the control β integrin subunits β_1 and β_3 (Fig. 4A, lanes 1, 3, and 5). Control blots incubated with anti-Myc antibody alone were negative (Fig. 4A, lanes 2, 4, and 6). Western blotting (Fig. 4A, lanes marked W) confirmed positions and equal loading amounts of the three β integrins. To further scrutinize the specificity of the β_4 /hCLCA2 adhesion, Far Western analyses were also conducted with blot-immobilized hCLCA2 (Fig. 4B, lane W) that was probed with soluble β_4 integrin immunopurified from MDA-MB-231 cell extracts. Binding of the β_4 integrin to hCLCA2 was confirmed by staining with anti- β_4 pAb H101 (Fig. 4B, lane 1), while blots that were stained with antibody alone in the absence of β_4 integrin were negative (Fig. 4B, lane 2).

Specificity of the β_4 Integrin/hCLCA2 Adhesion—The specificity of the β_4 integrin/hCLCA2 adhesion was confirmed by adhesion blocking experiments involving antibodies directed against either of the interacting adhesion molecules. Dramatic adhesion inhibition was seen only for anti-hCLCA2 pAb 18 and anti- β_4 mAb 3E1, while all other antibodies tested had no effect on the β_4 /hCLCA2 adhesion (Fig. 5, A and B). Neither of the two anti-hCLCA2 antibodies had any effect on the adhesion of MDA-MB-231 cells to human placenta-derived laminin used as

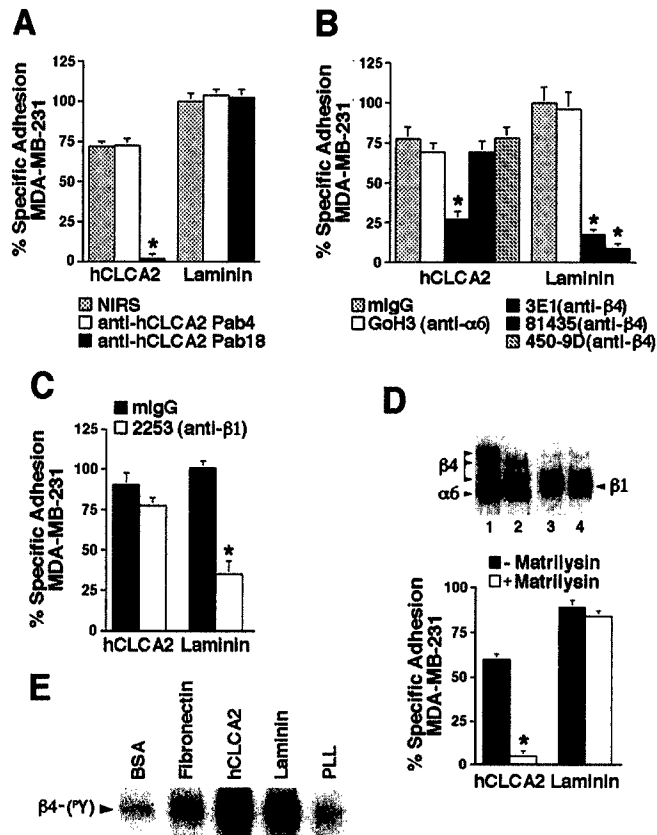


FIG. 5. Specificity of the β_4 integrin/hCLCA2 adhesion. A–C, MDA-MB-231/hCLCA2 and MDA-MB-231/laminin adhesion inhibition experiments were done in microtitration plates coated with 3 μ g/ml hCLCA2 or 7.5 μ g/ml placental laminin, using anti-hCLCA2 antibodies (pAbs 4 and 18) (A), anti- β_4 antibodies (3E1; 81435, 450-9D) and anti- α_6 antibodies (GoH3) (B), and functional anti- β_1 antibodies (2253) (C). Anti-hCLCA2 pAb 18 and anti- β_4 mAb 3E1 specifically block the adhesion of MDA-MB-231 to hCLCA2 but not anti- β_1 mAb 2253. D, matrilysin treatment of MDA-MB-231 cells abolishes adhesion to hCLCA2 but not to placental laminin and causes degradation of the 205-kDa β_4 integrin (Western blot, lane 2) but not the β_1 integrin (Western blot, lane 4). Western lanes 1 and 3 are untreated controls. E, MDA-MB-231 cancer cells were labeled in phosphate-free DMEM containing $\text{H}_3^{32}\text{PO}_4$ at a final concentration of 0.5 mCi/ml for 4 h at 37 °C and then seeded onto BSA (10 μ g/ml)-, fibronectin (5 μ g/ml)-, hCLCA2 (3 μ g/ml)-, placental laminin (7.5 μ g/ml)-, and poly-L-lysine (1 mg/ml)-coated dishes, incubated for 20 min at 37 °C, and lysed. Lysates were immunoprecipitated with anti- β_4 mAb 3E1, and precipitates were resolved by SDS-PAGE and treated with 1 M KOH for 2 h at 55 °C. Tyrosine-phosphorylated proteins are visualized by autoradiography. *, Student's *t* test; *p* < 0.01 (mean \pm S.D. from four experiments).

a control substrate, while both anti- β_4 antibodies 3E1 and 81435 inhibited laminin adhesion of MDA-MB-231 cells (Fig. 5, A and B). To exclude a possible participation of the $\alpha_6\beta_1$ integrin, expressed in all human breast cancer cell lines used in this study, in the hCLCA2 adhesion, functional anti- β_1 antibodies (mAb 2253) were tested and found to be ineffective in blocking the adhesion between MDA-MB-231 cells and hCLCA2 but effective in blocking the adhesion to placenta laminin (Fig. 5C).

In a second series of experiments, we show that selective cleavage of the β_4 integrin ectodomain with matrilysin (30) totally abolishes MDA-MB-231 adhesion to hCLCA2 yet had a negligible effect on the adhesion to placental laminin (Fig. 5D). These adhesion data were supported by Western analyses showing specific cleavage of the 205-kDa β_4 protein but not the β_1 integrin in matrilysin-treated tumor cells. Finally, we examined whether the MDA-MB-231 β_4 integrin was activated selectively when tumor cells were plated onto surfaces coated with hCLCA2 (Fig. 5E). Data showed prominent tyrosine phos-

phorylation of β_4 integrin in tumor cells bound to hCLCA2 and to placental laminin (31, 32). In contrast, fibronectin generated only a weak tyrosine phosphorylation reaction, and BSA and poly-L-lysine had no effect (Fig. 5E).

Lung Metastasis Is Inhibited by β_4 /hCLCA2 Adhesion-blocking Antibodies—To test whether the adhesion-inhibitory effects of anti-hCLCA2 and anti- β_4 integrin antibodies extended to an inhibition of lung metastasis, we performed lung colony assays in nude mice with the lung metastatic breast cancer cell line MDA-MB-231 in the presence of these antibodies. Prior to conducting these assays, we established that human MDA-MB-231 cells were able to adhere to mCLCA1 (Table I), the mouse counterpart of hCLCA2, and that this adhesion was inhibited with anti-Lu-ECAM-1 mAb 6D3 (22) (cross-reacts with mCLCA1) and anti- β_4 integrin mAb 3E1. Anti- β_4 mAb 3E1 was preincubated for 30 min and injected together with tumor cells, while mAb 6D3 was injected with tumor cells without preincubation. Control experiments were conducted in the presence of nonimmune mouse IgG. Mice sacrificed 15 weeks later revealed that both antibodies effectively blocked the colonization of the lungs by MDA-MB-231 cells, causing an 84% inhibition of lung metastasis with mAb 6D3 and a 100% inhibition with mAb 3E1 relative to mIgG-treated controls (Table I).

Effect of *in Vivo* Selection for Lung Metastatic Efficiency Versus β_4 Integrin Transfection—To test whether *in vivo* selection for increased lung metastatic performance was associated with increased β_4 expression, we compared the α_6 , β_1 , and β_4 expression patterns of the selected cell line MDA-MB-435L2 (20) with those of the parental MDA-MB-435 cell line and the β_4 -transfected MDA-MB-435 β_4 cell line (24). The parental MDA-MB-435 cell line exhibited strong expression of the α_6 and β_1 integrin subunits but only background levels of the β_4 integrin. Accordingly, these tumor cells adhered strongly to both placental and EHS laminins but poorly to hCLCA2 ($5 \pm 3\%$; Fig. 6A). The selected MDA-MB-435L2 expressed comparable levels of the α_6 and β_1 integrin subunits and a modest increase in surface expression of the β_4 integrin. In accordance with this expression pattern, MDA-MB-435L2 cells adhered strongly to the two laminins and exhibited an increased adhesion to hCLCA2 ($25 \pm 3\%$; Fig. 6A). These data were contrasted with those from the parental MDA-MB-435 cell line that had been transfected with human β_4 integrin and then selected for antibiotic resistance and by FACS for efficient stable expression of β_4 (24). Transfectant cells expressed significantly higher levels of β_4 integrin than MDA-MB-435L2 cells and adhered in higher numbers to hCLCA2 but in similar numbers to the two laminins, since the expression levels for both α_6 and β_1 remained unchanged. Transfection of MDA-MB-435 cells with tailless β_4 integrin ($\beta_4\Delta\text{cyt}$) underscored requirement of the “complete” β_4 integrin subunit in hCLCA2 binding, since adhesion to hCLCA2 did not improve relative to that of parental cells ($7 \pm 3\%$; Fig. 6A), albeit the expression level of the truncated β_4 was equal to that of wild-type β_4 expression in MDA-MB-231 cells. Consistent with published data, adhesion of $\beta_4\Delta\text{cyt}$ -transfected MDA-MB-435 cells to murine EHS laminin was also abolished (24), but not to human placental laminin (33).

As shown in Fig. 3, β_4 cell surface expression and hCLCA2 adhesion correlated well with lung colonization of the established cell lines MDA-MB-231, MDA-MB-435L2, and MDA-MB-435. Median and range of the number of lung colonies were 30 (5–100), 5 (0–17), and 0 (0–3), respectively. To our surprise, however, the β_4 -transfected cell line MDA-MB-435 β_4 was unable to produce lung colonies following a 15-week incubation period in nude mice, although the parental cell line MDA-MB-435 is known to produce lung metastases after orthotopic tu-

TABLE I
Inhibition of lung colonization by the human breast cancer cell line MDA-MB-231 with anti-mCLCA1 and anti- β_4 integrin antibodies

Cell line	Treatment	Adhesion to mCLCA1 ^a	Mice with lung metastases	Lung metastasis median (range) ^b
MDA-MB-231	mIgG ^c	65 ± 5	9/9	>100 (32-→100)
MDA-MB-231	mAb 6D3 ^d	9 ± 2	2/5	16 (0-38)
MDA-MB-231	mAb 3E1 ^e	8 ± 3	1/5	0 (0-1)

^a mCLCA1 was immunopurified from mCLCA1-transfected HEK293 cells using anti-Lu-ECAM-1 mAb 6D3.

^b Nude mice were injected via the lateral tail vein with 5×10^5 tumor cells/mouse/0.3 ml of DMEM in the presence of mouse nonimmune IgG, anti-Lu-ECAM-1 mAb 6D3, or anti- β_4 mAb 3E1, all at 200 μ g/mouse. Animals were sacrificed 15 weeks after tumor cell injection, and the number of lung colonies was counted under a dissecting microscope. Two mice in the mouse IgG-treated group died due to metastatic disease before termination of the experiment, the first at 8 weeks, the second at 12 weeks after injection of tumor cells.

^c Mouse nonimmune IgG.

^d Mouse anti-Lu-ECAM-1 mAb 6D3 cross-reacts with mCLCA1.

^e Mouse anti-human β_4 mAb 3E1.

mor growth in mammary fat pads of nude mice and *in vivo* selection of these cells yielded a cell line with transiently enhanced lung colonization potential (MDA-MB-435L2) (20), which was lost gradually with increasing passage number. To explore whether differences in the quality of the β_4 integrin expression on the surface of MDA-MB-231 and MDA-MB-435 β_4 cancer cells may have accounted for the discrepancy in the metastatic behavior, we examined the association between the β_4 integrin and its presumed α_6 partner in the two cell lines. Surface-biotinylated cancer cells were first subjected to immunoprecipitation with anti- β_4 pAb H101. As expected, the amounts of β_4 detected in streptavidin-HRP-probed blots were comparable with that identified by FACS (Fig. 6, A and B). Next, the same tumor cell extracts were subjected to immunoprecipitation with anti- α_6 mAb GoH3, and precipitates were analyzed for β_4 -co-immunoprecipitation. Surprisingly, only the β_4 of MDA-MB-231 cells was effectively co-precipitated with α_6 , while negligible amounts of β_4 were co-precipitated from MDA-MB-435 β_4 cells and none from MDA-MB-435 (Fig. 6B, lanes 1-3). Since $\beta_4\Delta$ cyt is also effectively co-immunoprecipitated with α_6 from MDA-MB-435 $\beta_4\Delta$ cyt extracts (Fig. 6B, lane 4), our data imply that wild-type β_4 transfected into MDA-MB-435 cells may interact with an intrinsic protein that affects co-immunoprecipitation with α_6 and metastasis but not *in vitro* adhesion to hCLCA2.

Transfection of Kirsten-Ras-transformed Balb/3T3 Cells with β_4 Promotes Adhesion to hCLCA2 and Lung Colonization—To determine whether overexpression of the β_4 integrin in a cell line that expresses low levels of β_4 integrin and, accordingly, has modest, yet consistent, lung metastatic capabilities, we chose a murine over a human tumor model. The former had the significant advantage that the metastatic performance could be tested in a syngeneic rather than a heterologous animal. Moreover, the induction time of generating macroscopically detectable lung colonies was only 3-4 weeks in syngeneic animals (13-15) versus a minimum of 15 weeks in a human/mouse model (20). The cell line we selected was the Kirsten-Ras-transformed Balb/3T3 cell line, which expressed low levels of the β_4 integrin and consistently produced a moderate number of lung colonies upon tail vein injection. These tumor cells were transfected with β_4 integrin cDNA or vector alone, and stable transfectants were selected based on antibiotic resistance. Expression of the β_4 integrin was confirmed by FACS and surface biotinylation, both methods indicating a significantly increased surface expression of β_4 integrin, which was co-immunoprecipitable with α_6 , in β_4 -transfected relative to vector-transfected cells (Fig. 7A). Prior to conducting a lung colony assay, adhesion assays were performed with mCLCA1, the mouse counterpart of hCLCA2. Adhesion of β_4 -transfected K-Balb cells to mCLCA1 was $66 \pm 5\%$ relative to $9 \pm 4\%$ for mock-transfected K-Balb cells (Fig. 7B). These adhesion data

paralleled the metastatic performance of the two cell lines. The β_4 -transfected K-Balb cells injected at 2×10^5 cells/mouse generated a median number of >100 colonies (69-→100), while the mock-transfected cell line only generated 24 (15-29) lung colonies (Fig. 7B). This difference was also reflected in the average lung weights of the two experimental groups, measuring 0.71 ± 0.22 g in β_4 transfectants and 0.45 ± 0.02 g in mock transfectants.

DISCUSSION

In this report, we describe a novel adhesion receptor/ligand pair that mediates colonization of the lungs by human breast cancer cells and possibly other cancer cell types. The pair consists of lung endothelial cell hCLCA2 and breast cancer cell β_4 integrin. Human CLCA2 is expressed by endothelia lining arterial and venous branches, all presumably derived from the bronchial artery, while prominent expression of the β_4 integrin has been associated with the invasive and metastatic phenotypes of breast cancer cells (24, 34-37). The location of MDA-MB-231 breast cancer metastases in mouse lungs is consistent with the vascular expression pattern of the mouse counterpart of hCLCA2 (mCLCA1) (10) as well as the recently established pattern of lung metastases by *in situ* epifluorescence microscopy (11). The binding interaction between the two lung metastasis-promoting adhesion molecules is documented by co-immunoprecipitation of the adhesion receptor/ligand pair from extracts of hCLCA2-transfected HEK293 monolayers to which MDA-MB-231 cells were bound, by hCLCA2 affinity chromatography, and by adhesion and metastasis inhibition experiments using functional antibodies. Participation of an "intermediary binding molecule" in the β_4 integrin/hCLCA2 adhesion was excluded by Far Western analyses, using blotted immunopurified β_4 or Myc-hCLCA2 and the corresponding purified adhesion partner as probe. Strong and specific binding between blotted β_4 integrin and Myc-hCLCA2 indicated that the β_4 integrin was able to recognize its endothelial cell receptor even after undergoing a vigorous denaturing/renaturing treatment, suggesting that the usually required interaction between α and β integrin subunits (38, 39) and/or other interacting cell surface and intracellular molecules (40, 41) is not a mandate for the β_4 integrin/hCLCA2 adhesion function *in vitro*. This behavior is similar to that recently reported for the β_4 integrin/Shc adhesion, using blotted β_4 integrin under denaturing/renaturing Far Western conditions (42).

Molecular cloning of hCLCA2 from a lung cDNA library and biochemical and functional characterization of hCLCA2 protein have shown that the molecule shares many of the characteristics of the other CLCA family members (18). The adhesion function of CLCA channel proteins is perplexing but not without precedent. Studies involving the cystic fibrosis transmembrane conductance regulator have shown that this chloride

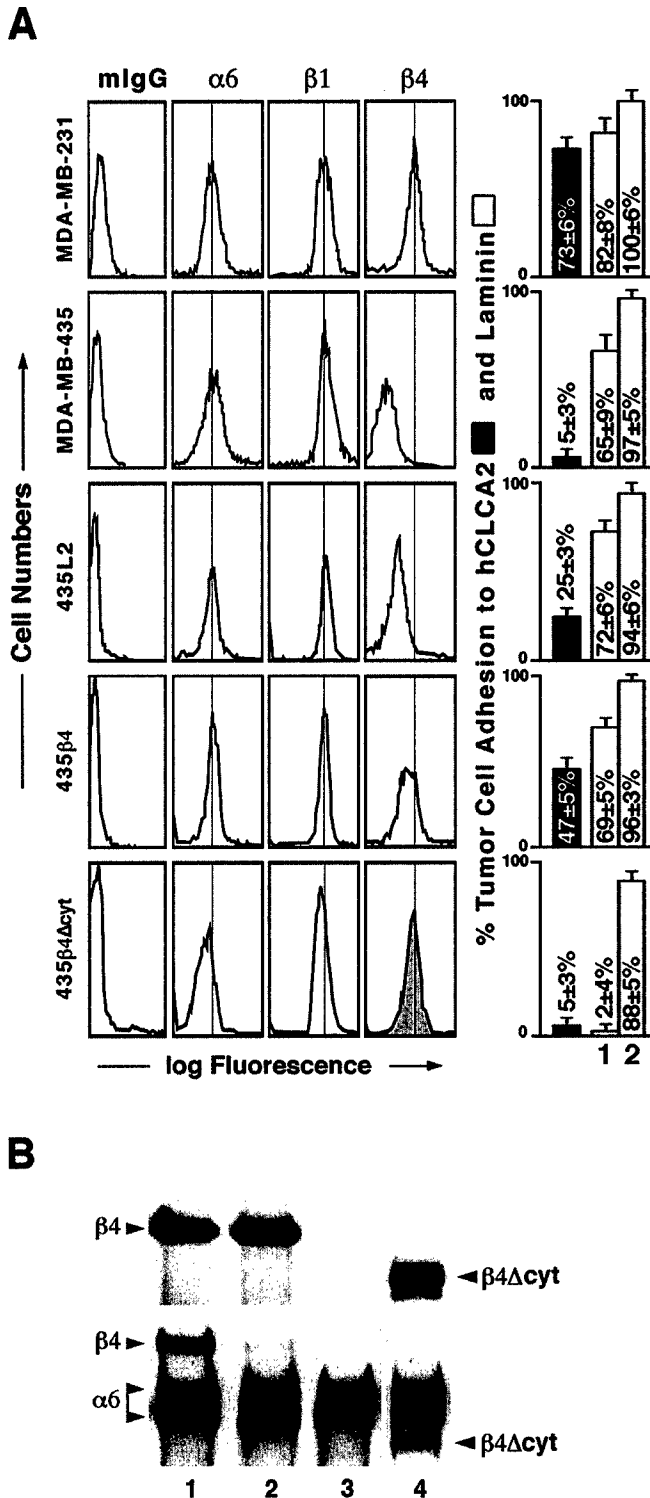


FIG. 6. Effect of *in vivo* selection versus β_4 -transfection on hCLCA2 adhesion of human breast cancer cells. A, MDA-MB-231, MDA-MB-435, MDA-MB-435L2, MDA-MB-435 β_4 , and MDA-MB-435 $\beta_4\Delta$ cyt were analyzed for α_6 , β_1 , and β_4 expression by FACS, and the expression patterns were contrasted with adhesion to hCLCA2 and EHS (bars 1) and placental (bars 2) laminins (coated at 3 μ g/ml, 20 μ g/ml, and 7.5 μ g/ml, respectively). *In vivo* selection of MDA-MB-435 for enhanced lung colonization (MDA-MB-435L2) (20) and stable β_4 transfection of MDA-MB-435 (MDA-MB-435 β_4) (24) increases β_4 expression and adhesion to hCLCA2, while adhesion to the two laminins remains unchanged. Stable transfection of MDA-MB-435 with tailless β_4 (MDA-MB-435 $\beta_4\Delta$ cyt) (24) increases β_4 expression as detected with anti- β_4 mAb 3E1 (directed against the extracellular domain of the β_4 integrin), but $\beta_4\Delta$ cyt-transfectants adhere in similarly poor numbers to hCLCA2 as parental cells. Adhesion of MDA-MB-435 $\beta_4\Delta$ cyt to EHS laminin (bar 1) is abolished, but not adhesion to placental laminin (bar

channel protein is also a cellular adhesion receptor for *Pseudomonas aeruginosa* (16) and *Salmonella typhi* (17). In cancer metastasis, a novel concept is the possible involvement of a CLCA-mediated Cl^- conductance in cancer cell extravasation by induction of apoptosis in the endothelium of the target organ. Support for such involvement came from recent observations that breast cancer cells seeded atop a monolayer of hCLCA2-expressing HUVEC apparently induce apoptosis in apposed endothelial cells (43). Endothelial apoptosis appears to involve expression and activation of chloride channels (44, 45), leading to intracellular acidification and, in turn, activation of endonucleases and chromatin digestion (44). The advantage of a selective induction of apoptosis in those endothelial cells to which tumor cells are bound is obvious, since reduction of the endothelial cell by apoptotic vesiculation may create an avenue for invasion of perivascular tissues by tumor cells. The notion that these events are initiated by β_4 /hCLCA2 adhesion is supported by our preliminary observation that endothelial cells incubated with immunopurified β_4 integrin rapidly undergo apoptosis. The apoptotic index of β_4 -treated endothelial cells was 26%, relative to 4% in untreated endothelial cells.²

The β_4 integrin has previously been linked to metastatic disease (13, 46–49) and is confirmed here as a lung metastasis-associated gene in breast cancer. Consistent with the involvement of multiple genes in metastasis (1–8), the β_4 integrin, like other metastasis-associated genes including MMP-2, CD44, $\alpha_v\beta_3$ integrin, and α_6 integrin (50), is by itself incapable of conferring mastery of the complex, multistep cascade of metastasis. This is exemplified by the MDA-MB-468 breast cancer cell line, which expresses the $\alpha_6\beta_4$ integrin at relatively high levels and, accordingly, is able to adhere to hCLCA2 *in vitro* but fails to produce metastases upon tail vein inoculation (Fig. 3). When this cell line is compared with a metastatically competent, β_4 -expressing cell line such as MDA-MB-231, the former expresses a phenotype that is comparable with the spontaneously immortalized, nontumorigenic β_4 integrin-expressing breast epithelial cell line MFC-10A (51), while the latter expresses an aggressive, invasive, and metastatic phenotype (20). This difference is manifested by the formation of a contact-inhibited, cobblestone-like monolayer *in vitro* and adenomatous growth *in vivo* by MDA-MB-468 cells but anaplastic, crisscrossed, and multilayered growth *in vitro* and the formation of invasive and metastatic tumors *in vivo* by MDA-MB-231 cells (20). Genotype analyses indicate that the latter cell line expresses an array of gene abnormalities that have been associated with metastasis such as overexpression of *c-erbB-2* (52), *MTA1* (53, 54), *MT1-MMP* (55), vimentin (56), α_6 integrin (57), and *VEGF* (58) and down-regulation or loss of E-cadherin (59), *nm23-H1* (60), and *MUC1* (61), while most of these genes are expressed at normal or near normal levels in MDA-MB-468 cells (50, 53, 55, 56, 62). These data imply that β_4 integrin expression leads to lung metastasis only in those cancer cells possessing a genotype that is otherwise compatible with metastasis. A similar scenario as described for the β_4 integrin has also been reported for other metastasis-associated proteins including MMP-2, CD44, $\alpha_v\beta_3$ integrin, α_6 integrin, Rho

² B. U. Pauli, H.-C. Cheng, and M. Abdel-Ghany, manuscript in preparation.

2). B, extracts from surface-biotinylated MDA-MB-231, MDA-MB-435 β_4 , MDA-MB-435 $\beta_4\Delta$ cyt, and MDA-MB-435 cells were subjected to immunoprecipitation with anti- β_4 pAb H101 (upper panel) or anti- α_6 mAb GoH3 (lower panel). Immunoprecipitates were resolved by SDS-PAGE (6%) and blotted to nitrocellulose and then probed with Streptavidin-HRP. Lane 1, MDA-MB-231; lane 2, MDA-MB-435 β_4 ; lane 3, MDA-MB-435; lane 4, MDA-MB-435 $\beta_4\Delta$ cyt.

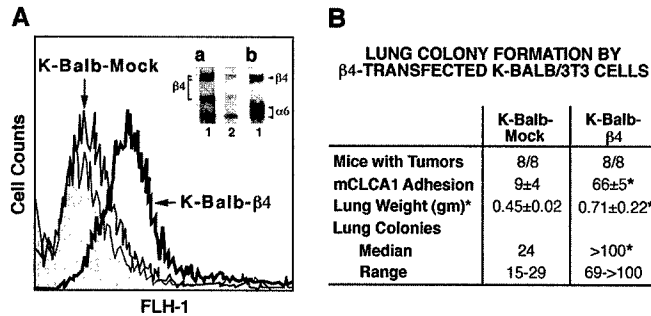


FIG. 7. Effect of stable β_4 transfection of K-Balb/3T3 cells on mCLCA1 adhesion and lung colony formation. A, Kirsten-Ras-transformed Balb/3T3 (K-Balb/3T3) cells were transfected by electroporation with β_4 integrin cDNA, and stable expressors were selected by G418 resistance. Wild-type K-Balb/3T3 cells (gray filled histogram), mock-transfected K-Balb/3T3 cells (thin open histogram), and β_4 -transfected K-Balb/3T3 cells (thick open histogram) were stained with rabbit anti- β_4 pAb H101 and fluorescein isothiocyanate-conjugated goat anti-rabbit IgG secondary antibody and then analyzed by FACS. Inset, anti- β_4 pAb H101 immunoprecipitates from extracts of surface-biotinylated β_4 -transfected K-Balb/3T3 cells (a, lane 1) and mock-transfected K-Balb/3T3 cells (a, lane 2) and anti- α_6 mAb GoH3 immunoprecipitates from surface-biotinylated, β_4 -transfected K-Balb/3T3 cells (b, lane 1). B, lung colony formation by β_4 -transfected K-Balb/3T3 cells. Balb/c mice (6-weeks old; male) were injected into the lateral tail vein with 2×10^6 tumor cells plus 0.3 ml of DMEM/mouse, and lung weights (g) and number of lung colonies were determined 3 weeks after tumor cell injection. Data were evaluated by Student's *t* test (unpaired data). *, $p < 0.01$ (relative to K-Balb-Mock).

GTPases, and fibronectin, which are prominently expressed in many highly invasive and metastatic tumor cells but individually are also detected in benign, nonmetastatic tumor cells and even normal cells (25, 63–67).

While an early stage of tumor progression (benign, well differentiated tumor) may have accounted for lack of metastasis in β_4 -expressing MDA-MB-468 cells, an altered modulation of the β_4 integrin by lateral associations with other membrane (and/or cytoplasmic) proteins (reviewed in Refs. 40 and 41) in β_4 -transfected MDA-MB-435 cells versus MDA-MB-231 cells may have been responsible for the observed discrepancy in the metastatic behavior of the two cell lines. Although we have as yet no evidence of such a differential lateral association of the β_4 integrin in the two cell lines, we show here that anti- α_6 antibodies fail to co-immunoprecipitate the β_4 integrin from β_4 -transfected MDA-MB-435 cell extracts but effectively do so from MDA-MB-231 cell extracts (as well as from extracts of immortalized normal breast epithelial cells MCF-10A and benign breast tumor cells MDA-MB-468; data not shown). This differential partitioning of the β_4 integrin in MDA-MB-231 and MDA-MB-435 β_4 cells, which incidentally express virtually identical amounts of α_6 and β_1 integrins, and only a slightly reduced level of β_4 in the MDA-MB-435 β_4 cell line is difficult to explain. However, it is possible that under our extraction conditions (1% Triton X-100), lateral association of the β_4 integrin with an as yet undetermined membrane or cytoplasmic protein in β_4 -transfected MDA-MB-435 cells may have weakened the binding interaction between the α_6 and β_4 integrin subunits, resulting not only in failure of the two integrin subunits to co-immunoprecipitate but also in inability to metastasize. Control co-immunoprecipitation of α_6 and $\beta_4\Delta$ cyt suggests that such association is mediated by the cytoplasmic tail of the β_4 integrin. Alternatively, our data may have been affected by the unlikely event that the β_4 integrin subunit may associate with an as yet unidentified α chain to permit cell surface expression in β_4 -transfected MDA-MB-435 tumor cells.

These considerations have important experimental consequences for metastasis research, since transfection of a gene suspected to play a primary role in metastasis into a tumor cell

line that is nonmetastatic may not yield the expected result, since the introduced gene, even if it appropriately associates with other membrane proteins to achieve proper function, may not be sufficient in ending tumors with mastery over the complete metastatic cascade. Therefore, we have relied in our transfection studies on a cell line that has a low lung metastatic potential and, thus, expresses a gene array that is conducive to lung metastasis including a low level of β_4 integrin expression. When the β_4 integrin is overexpressed in these cells, the number of lung colonies generated from intravenously injected tumor cells increases proportional to the level of α_6 co-immunoprecipitable β_4 integrin. Consistent with involvement of the β_4 integrin gene in metastasis, blockage of the β_4 /hCLCA2 adhesion abrogates metastasis. Similar effects are achieved by blocking other metastasis-associated genes each facilitating a different step in the metastatic cascade, e.g. RhoC, metalloproteinases, heparinase, angiogenic factors, dipeptidyl peptidase IV (68–75).

In conclusion, we have provided molecular evidence in support of the observed link between β_4 expression and malignant progression (reviewed in Ref. 21), ascribing a key role to the adhesion mechanism between β_4 integrin and vascular endothelial cell hCLCA2 in lung metastasis. Although only a few examples of integrin involvement in cell-to-cell adhesion are known (e.g. leukocyte integrins $\alpha_L\beta_2$ and $\alpha_M\beta_2$ bind to endothelial cell ICAM-1, integrins $\alpha_4\beta_1$ and $\alpha_7\beta_1$ to VCAM-1, and $\alpha E\beta 7$ to E-cadherin (reviewed in Ref. 39)), we have identified and cloned for the first time a β_4 integrin-binding protein that is an integral membrane protein and that is entirely new as an integrin-binding partner (15, 18). Our discovery that hCLCA2 has an important function in heterotypic cell-to-cell adhesion in addition to that in Ca^{2+} -sensitive chloride conductance extends the basic knowledge about this protein and indicates that ion channels can have multiple, seemingly unrelated functions (16–18, 44, 76).

Acknowledgment—We thank Dr. Renée A. Christopher for involvement in the preparation of the manuscript and Heather Archibald and the staff of the Image Lab for expert technical assistance.

REFERENCES

- Zhang, L., Zhou, W., Velculescu, V. E., Kern, S. E., Hruban, R. H., Hamilton, S. R., Vogelstein, B., and Kinzler, K. W. (1997) *Science* **276**, 1268–1272
- Perou, C. M., Sorlie, T., Eisen, M. B., van de, R. M., Jeffrey, S. S., Rees, C. A., Pollack, J. R., Ross, D. T., Johnsen, H., Akslen, L. A., Fluge, O., Pergamenschikov, A., Williams, C., Zhu, S. X., Lonning, P. E., Borresen-Dale, A. L., Brown, P. O., and Botstein, D. (2000) *Nature* **406**, 747–752
- Hanahan, D., and Weinberg, R. A. (2000) *Cell* **100**, 57–70
- Fidler, I. J. (2000) *Cancer J. Sci. Am.* **6**, Suppl. 2, 134–141
- Shain, K. H., Landowski, T. H., and Dalton, W. S. (2000) *Curr. Opin. Oncol.* **12**, 557–563
- Zetter, B. R. (1993) *Semin. Cancer Biol.* **4**, 219–229
- Pauli, B. U., and Lin, H. (1997) in *Encyclopedia of Cancer* (Bertino, J. R., ed) Vol. 1, pp. 464–476, Academic Press, Inc., San Diego
- Orr, F. W., Wang, H. H., Lafrenie, R. M., Scherbarth, S., and Nance, D. M. (2000) *J. Pathol.* **190**, 310–329
- Goetz, D. J., el Sabban, M. E., Hammer, D. A., and Pauli, B. U. (1996) *Int. J. Cancer* **65**, 192–199
- Zhu, D., and Pauli, B. U. (1993) *Int. J. Cancer* **53**, 628–633
- Al Mehdi, A. B., Tozawa, K., Fisher, A. B., Shientag, L., Lee, A., and Muschel, R. J. (2000) *Nat. Med.* **6**, 100–102
- Pauli, B. U., and Lee, C. L. (1988) *Lab. Invest.* **58**, 379–387
- Zhu, D. Z., Cheng, C. F., and Pauli, B. U. (1991) *Proc. Natl. Acad. Sci. U. S. A.* **88**, 9568–9572
- Zhu, D., Cheng, C. F., and Pauli, B. U. (1992) *J. Clin. Invest.* **89**, 1718–1724
- Elble, R. C., Widom, J., Gruber, A. D., Abdel-Ghany, M., Levine, R., Goodwin, A., Cheng, H. C., and Pauli, B. U. (1997) *J. Biol. Chem.* **272**, 27853–27861
- Pier, G. B., Grout, M., and Zaidi, T. S. (1997) *Proc. Natl. Acad. Sci. U. S. A.* **94**, 12088–12093
- Pier, G. B., Grout, M., Zaidi, T., Meluleni, G., Mueschenborn, S. S., Banting, G., Ratcliff, R., Evans, M. J., and Colledge, W. H. (1998) *Nature* **393**, 79–82
- Pauli, B. U., Abdel-Ghany, M., Cheng, H. C., Gruber, A. D., Archibald, H. A., and Elble, R. C. (2000) *Clin. Exp. Pharmacol. Physiol.* **27**, 901–905
- Gruber, A. D., Schreier, K. D., Ji, H. L., Fuller, C. M., and Pauli, B. U. (1999) *Am. J. Physiol.* **276**, C1261–C1270
- Price, J. E. (1996) *Breast Cancer Res. Treat.* **39**, 93–102
- Rabinovitz, I., and Mercurio, A. M. (1996) *Biochem. Cell Biol.* **74**, 811–821
- Zhu, D. Z., and Pauli, B. U. (1991) *J. Histochem. Cytochem.* **39**, 1137–1142

23. Kemperman, H., Wijnands, Y., de Rijk, D., and Roos, E. (1993) *Cancer Res.* **53**, 3611-3617
24. Shaw, L. M., Chao, C., Wewer, U. M., and Mercurio, A. M. (1996) *Cancer Res.* **56**, 959-963
25. Cheng, H. C., Abdel-Ghany, M., Elble, R. C., and Pauli, B. U. (1998) *J. Biol. Chem.* **273**, 24207-24215
26. Giancotti, F. G., Stepp, M. A., Suzuki, S., Engvall, E., and Ruoslahti, E. (1992) *J. Cell Biol.* **118**, 951-959
27. Potts, A. J., Croall, D. E., and Hemler, M. E. (1994) *Exp. Cell Res.* **212**, 2-9
28. Abdel-Ghany, M., Kole, H. K., and Racker, E. (1987) *Proc. Natl. Acad. Sci. U. S. A.* **84**, 8888-8892
29. Aguirre, K. M., McCormick, R. J., and Schwarzbauer, J. E. (1994) *J. Biol. Chem.* **269**, 27863-27868
30. von Bredow, D. C., Nagle, R. B., Bowden, G. T., and Cress, A. E. (1997) *Exp. Cell Res.* **236**, 341-345
31. Mainiero, F., Pepe, A., Wary, K. K., Spinardi, L., Mohammadi, M., Schlessinger, J., and Giancotti, F. G. (1995) *EMBO J.* **14**, 4470-4481
32. Mainiero, F., Pepe, A., Yeon, M., Ren, Y., and Giancotti, F. G. (1996) *J. Cell Biol.* **134**, 241-253
33. Spinardi, L., Einheber, S., Cullen, T., Milner, T. A., and Giancotti, F. G. (1995) *J. Cell Biol.* **129**, 473-487
34. Jones, J. L., Royall, J. E., Critchley, D. R., and Walker, R. A. (1997) *Exp. Cell Res.* **235**, 325-333
35. Falcioni, R., Antonini, A., Nistico, P., Di Stefano, S., Crescenzi, M., Natali, P. G., and Sacchi, A. (1997) *Exp. Cell Res.* **236**, 76-85
36. O'Connor, K. L., Shaw, L. M., and Mercurio, A. M. (1998) *J. Cell Biol.* **143**, 1749-1760
37. Gambaletta, D., Marchetti, A., Benedetti, L., Mercurio, A. M., Sacchi, A., and Falcioni, R. (2000) *J. Biol. Chem.* **275**, 10604-10610
38. Loftus, J. C., and Liddington, R. C. (1997) *J. Clin. Invest.* **99**, 2302-2306
39. Plow, E. F., Haas, T. A., Zhang, L., Loftus, J., and Smith, J. W. (2000) *J. Biol. Chem.* **275**, 21785-21788
40. Hemler, M. E. (1998) *Curr. Opin. Cell Biol.* **10**, 578-585
41. Woods, A., and Couchman, J. R. (2000) *J. Biol. Chem.* **275**, 24233-24236
42. Dans, M., Gagnoux-Palacios, L., Blaikie, P., Klein, S., Mariotti, A., and Giancotti, F. G. (2001) *J. Biol. Chem.* **276**, 1494-1502
43. Kebers, F., Lewalle, J. M., Desreux, J., Munaut, C., Devy, L., Foidart, J. M., and Noel, A. (1998) *Exp. Cell Res.* **240**, 197-205
44. Szabo, I., Lepple-Wienhues, A., Kaba, K. N., Zoratti, M., Gulbins, E., and Lang, F. (1998) *Proc. Natl. Acad. Sci. U. S. A.* **95**, 6169-6174
45. Gottlieb, R. A., and Dosanjh, A. (1996) *Proc. Natl. Acad. Sci. U. S. A.* **93**, 3587-3591
46. Falcioni, R., Kennel, S. J., Giacomini, P., Zupi, G., and Sacchi, A. (1986) *Cancer Res.* **46**, 5772-5778
47. Perrotti, D., Cimino, L., Falcioni, R., Tibursi, G., Gentileschi, M. P., and Sacchi, A. (1990) *Anticancer Res.* **10**, 1587-1597
48. Rossen, K., Dahlstrom, K. K., Mercurio, A. M., and Wewer, U. M. (1994) *Acta Dermato-Venereologica* **74**, 101-105
49. Cimino, L., Perrotti, D., D'Agostino, G., Falcioni, R., and Sacchi, A. (1997) *Cancer Detect. Prev.* **21**, 158-166
50. Roetger, A., Merschjann, A., Dittmar, T., Jackisch, C., Barnekow, A., and Brandt, B. (1998) *Am. J. Pathol.* **153**, 1797-1806
51. Soule, H. D., Maloney, T. M., Wolman, S. R., Peterson, W. D., Brenz, R., McGrath, C. M., Russo, J., Pauley, R. J., Jones, R. F., and Brooks, S. C. (1990) *Cancer Res.* **50**, 6075-6086
52. Lee-Huang, S., Huang, P. L., Sun, Y., Chen, H. C., Kung, H. F., Huang, P. L., and Murphy, W. J. (2000) *Anticancer Res.* **20**, 653-659
53. Toh, Y., Pencil, S. D., and Nicolson, G. L. (1995) *Gene (Amst.)* **159**, 97-104
54. Nawa, A., Nishimori, K., Lin, P., Maki, Y., Moue, K., Sawada, H., Toh, Y., Fumitaka, K., and Nicolson, G. L. (2000) *J. Cell. Biochem.* **78**, 202-212
55. Pulyaeva, H., Bueno, J., Polette, M., Birembaut, P., Sato, H., Seiki, M., and Thompson, E. W. (1997) *Clin. Exp. Metastasis* **15**, 111-120
56. Thompson, E. W., Paik, S., Brunner, N., Sommers, C. L., Zugmaier, G., Clarke, R., Shima, T. B., Torri, J., Donahue, S., Lippman, M. E., Martin, G. R., and Dickson, R. B. (1992) *J. Cell. Physiol.* **150**, 534-544
57. Mukhopadhyay, R., Theriault, R. L., and Price, J. E. (1999) *Clin. Exp. Metastasis* **17**, 325-332
58. Donovan, D., Harmey, J. H., Toomey, D., Osborne, D. H., Redmond, H. P., and Bouchier-Hayes, D. J. (1997) *Ann. Surg. Oncol.* **4**, 621-627
59. Mbalaviele, G., Dunstan, C. R., Sasaki, A., Williams, P. J., Mundy, G. R., and Yoneda, T. (1996) *Cancer Res.* **56**, 4063-4070
60. Russell, R. L., Geisinger, K. R., Mehta, R. R., White, W. L., Shelton, B., and Kute, T. E. (1997) *Cancer* **79**, 1158-1165
61. Walsh, M. D., Luckie, S. M., Cummings, M. C., Antalis, T. M., and McGuckin, M. A. (1999) *Breast Cancer Res. Treat.* **58**, 255-266
62. Hazan, R. B., and Norton, L. (1998) *J. Biol. Chem.* **273**, 9078-9084
63. Bohm, J. P., Niskanen, L. K., Pirinen, R. T., Kiraly, K., Kellokoski, J. K., Moisio, K. I., Eskelinen, M. J., Tulla, H. E., Hollmen, S., Alhava, E. M., and Kosma, V. M. (2000) *J. Pathol.* **192**, 321-327
64. Fritz, G., Just, I., and Kaina, B. (1999) *Int. J. Cancer* **81**, 682-687
65. Hofmann, U. B., Westphal, J. R., van Muijen, G. N., and Ruitter, D. J. (2000) *J. Invest. Dermatol.* **115**, 337-344
66. Maguire, P. D., Qi, W., Lallemand, R., and Scully, S. P. (2000) *Oncology* **59**, 139-144
67. Taverna, D., Ullman-Cullere, M., Rayburn, H., Bronson, R. T., and Hynes, R. O. (1998) *Cancer Res.* **58**, 848-853
68. Clark, E. A., Golub, T. R., Lander, E. S., and Hynes, R. O. (2000) *Nature* **406**, 532-535
69. Curran, S., and Murray, G. I. (2000) *Eur. J. Cancer* **36**, 1621-1630
70. Hulett, M. D., Freeman, C., Hamdorf, B. J., Baker, R. T., Harris, M. J., and Parish, C. R. (1999) *Nat. Med.* **5**, 803-809
71. Vlodaysky, I., Friedmann, Y., Elkin, M., Aingorn, H., Atzmon, R., Ishai-Michaeli, R., Bitan, M., Pappo, O., Peretz, T., Michal, I., Spector, L., and Pecker, I. (1999) *Nat. Med.* **5**, 793-802
72. Bergers, G., Javaherian, K., Lo, K. M., Folkman, J., and Hanahan, D. (1999) *Science* **284**, 808-812
73. Yip, D., Ahmad, A., Karapetis, C. S., Hawkins, C. A., and Harper, P. G. (1999) *Invest. New Drugs* **17**, 387-399
74. O'Reilly, M. S., Holmgren, L., Shing, Y., Chen, C., Rosenthal, R. A., Moses, M., Lane, W. S., Cao, Y., Sage, E. H., and Folkman, J. (1994) *Cell* **79**, 315-328
75. Abdel-Ghany, M., Cheng, H., Levine, R. A., and Pauli, B. U. (1998) *Invasion Metastasis* **18**, 35-43
76. Martin, D. K., Boneham, G. C., Pirie, B. L., Collin, H. B., and Campbell, T. J. (1996) *Microvasc. Res.* **52**, 200-209



DEPARTMENT OF THE ARMY
US ARMY MEDICAL RESEARCH AND MATERIEL COMMAND
504 SCOTT STREET
FORT DETRICK, MARYLAND 21702-5012

REPLY TO
ATTENTION OF:

MCMR-RMI-S (70-1y)

26 Nov 02

MEMORANDUM FOR Administrator, Defense Technical Information
Center (DTIC-OCA), 8725 John J. Kingman Road, Fort Belvoir,
VA 22060-6218

SUBJECT: Request Change in Distribution Statement

1. The U.S. Army Medical Research and Materiel Command has reexamined the need for the limitation assigned to technical reports written for this Command. Request the limited distribution statement for the enclosed accession numbers be changed to "Approved for public release; distribution unlimited." These reports should be released to the National Technical Information Service.

2. Point of contact for this request is Ms. Kristin Morrow at DSN 343-7327 or by e-mail at Kristin.Morrow@det.amedd.army.mil.

FOR THE COMMANDER:

A handwritten signature in black ink, appearing to read "Phyllis M. Rinehart", is written over the typed name and title.

PHYLIS M. RINEHART
Deputy Chief of Staff for
Information Management

Encl

ADB263708
ADB257291
ADB262612
ADB266082
ADB282187
ADB263424
ADB267958
ADB282194
ADB261109
ADB274630
ADB244697
ADB282244
ADB265964
ADB248605
ADB278762
ADB264450
ADB279621
ADB261475
ADB279568
ADB262568
ADB266387
ADB279633
ADB266646
ADB258871
ADB266038
ADB258945
ADB278624